Marine Environmental Research 212 (2025) 107587

Contents lists available at ScienceDirect

Marine Environmental Research

journal homepage: www.elsevier.com/locate/marenvrev

On a trawled north Pacific seamount, reductions of benthic megafauna abundance, diversity, and ecosystem function are correlated with increased evidence of fishing

Virginia C. Biede [a], Nicole B. Morgan [a], E. Brendan Roark [b], Amy R. Baco [a,*]

[a] Department of Earth, Ocean, And Atmospheric Science, Florida State University, 1011 Academic Way, Tallahassee, FL, 32306, USA
[b] Department of Geography, Texas A&M University, College Station, TX, 77843-3147, USA

ARTICLE INFO

Keywords:
Vulnerable marine ecosystems
Significant adverse impacts
Biodiversity
Functional traits
Disturbance
Recovery
Resilience

ABSTRACT

High-seas seamounts in the Hawaiian-Emperor Seamount Chain are exposed to bottom-contact fisheries, i.e., historical and contemporary trawl, coral tangle net, longline, and gillnet fisheries, that disturb vulnerable marine ecosystem megafauna, such as deep-sea corals and sponges. Koko Guyot is the largest of these features and has experienced destructive fishing practices for more than half a century. To better understand the state of vulnerable megafaunal communities on Koko, the submersibles *Pisces IV* and *V* obtained high-quality imagery from replicate transects of 500 m length at two sites along 400, 500, and 600 m depth contours. Visual evidence of fishing, trawl scars and anthropogenically sourced debris, were compared to the abundance, diversity, and ecosystem function of benthic megafauna. Multiple faunal assemblages were observed, ranging from depauperate communities dominated by sea urchins and cup corals to diverse coral gardens with octocorals and scleractinian reef-forming species. Overall, megafaunal abundance, diversity, and metrics of ecosystem function were significantly negatively correlated with increased visual evidence of fishing. Coralliid octocorals were previously targeted by fisheries on the seamount chain and were found in low abundance on Koko, supporting the evidence for disturbance. Yet the pockets of diverse octocoral gardens with small colonies of reef-forming scleractinian species support the presence of remnant or recovering populations. Therefore, Koko appears to host a mosaic of disturbed, recovering, and remnant communities requiring protection from future disturbance. This study highlights the importance of fine-scale analyses for assessing disturbed, remnant and recovering communities.

1. Introduction

Globally, approximately 60 % of seamounts are exposed to fishing activity, with 57 % targeted by longline fisheries and 7 % targeted by trawling fisheries (Kerry et al., 2022). Despite this, the resilience of the diverse resident seamount benthic communities is poorly understood. This is of particular concern for fisheries management because rich biogenic habitats and vulnerable marine ecosystems (VMEs) are often associated with seamounts. These diverse ecosystems include cold-water coral reefs, coral gardens, and sponge grounds that can be easily removed and fragmented by bottom-contact fishing pressure (Baco et al., 2019; Morgan and Baco, 2020; Buhl-Mortensen et al., 2010; Clark et al., 2019; Colaço et al., 2022; Waller et al., 2007; Watling and Norse, 1998; Yoklavich et al., 2018). Thus, these features are important regional fishing grounds, but also critical biodiversity hotspots (reviewed in Freiwald et al., 2004; Rogers, 2018).

On seamounts of the Hawaiian-Emperor Seamount Chain (HESC), significant bottom-contact fishing efforts (i.e., trawling, coral tangle net, long-line, and gillnet fisheries) from the 1960s to 1980s targeted precious corals, as well as finfishes, primarily pelagic armourhead (*Pentaceros wheeleri*) and splendid alfonsino (*Beryx splendens*) (Grigg, 2002; Clark et al., 2007). Unfortunately, historical fishing effort has been difficult to track within seamounts, as the historical methods of tracking catch data only relayed regional effort (e.g., Tsounis et al., 2010; Uchida et al., 1986). At a global scale, the HESC seamounts cumulatively have experienced a larger number of fishing hours than any other fished seamounts (Kerry et al., 2022; Clark et al., 2007). Current fishing effort on the HESC has been reduced to a small number of vessels and to seamounts outside of the Papahānaumokuākea National Marine Sanctuary. Bottom-contact fishing leaves persistent

* Corresponding author.
E-mail address: abacotaylor@fsu.edu (A.R. Baco).

https://doi.org/10.1016/j.marenvres.2025.107587
Received 6 June 2025; Received in revised form 26 September 2025; Accepted 28 September 2025
Available online 29 September 2025

impacts on the seafloor itself and on seafloor communities in the form of trawl scars, lost weights, netting and lines, along with loss of biomass, loss of richness, and loss of habitat heterogeneity that does not recover in 5–15 years (Clark et al., 2019; Waller et al., 2007; Althaus et al., 2009; Williams et al., 2001, 2010). Bottom trawling specifically removes the sessile communities in the path of the trawling gear, resuspends particulates that can choke surrounding suspension feeders, removes targeted and bycatch fauna from the food web (e.g., Clark et al., 2016; Watling and Norse, 1998), and can lead to reduced heterogeneity of seafloor morphology (Puig et al., 2012). Whereas lost gear from multiple fisheries can damage habitats through continued ghost fishing and entanglement (Gilman et al., 2021). Areas exposed to fishing pressure and derelict gear have more fragmented and missing corals (Yoklavich et al., 2018; Stone, 2006), exhibiting signs of significant adverse impacts (SAI). These SAIs are defined as fishing impacts with the capacity to alter ecosystem structure and/or function, e.g., removing rare, fragile, or long-lived organisms, decreasing the three-dimensional structure of communities to rubble (FAO, 2009). Unfortunately, SAIs have been observed on all studied seamounts currently and historically exposed to fishing pressure in the HESC (Baco et al., 2019, 2020, 2023a).

However, the process of recovery is evident on several HESC seamounts that were previously trawled and have remained undisturbed for the past 40 years (Baco et al., 2019, 2023a). Recovery from disturbance can include multiple community states before reaching an alternate state or returning to the pre-disturbance state (reviewed in Lotze et al., 2011). A disturbed state is often characterized by exceptionally low abundances or the absence of taxa not resistant to the disturbance (Lotze et al., 2011; Connell, 1978). Studies using imagery focusing on epibenthic hard substrate communities have found evidence that trawling resistance is limited to small and or flexible specimens within seamount communities (reviewed in Goode et al., 2020). From the disturbed state, the process of recovery requires some forward progression towards the original community, such as an increase in diversity metrics or abundance (Lotze et al., 2011). This might include early colonizers and rapid growers, as well as resistant and remnant taxa observed in the disturbed state. Such progress has been observed in the HESC seamounts through increased faunal abundance on seamounts protected for 30–40 years in comparison to seamounts still experiencing fishing pressure (Baco et al., 2019). In terms of recovering to the original state, the precious corals, *Pleurocorallium secundum* and *Hemicorallium laauense*, once targeted by the fishing industry in the same region, showed evidence of remnant or recovering populations on select sites, with Koko Guyot as one site with potentially recovering *H. laauense* populations (Baco et al., 2023a).

Koko Guyot is the largest non-emergent seamount of the HESC and has been exposed to significant fishing effort since the 1960s (Morgan and Baco, 2020; Clark et al., 2007; Clague et al., 1980). Located near the bend of the HESC and inhabited by both Alaskan fauna and Hawaiian fauna, Koko is noted for high regional biodiversity. Koko hosts a rich community of corals and benthic fauna including particularly diverse octocoral assemblages (Miyamoto et al., 2017; Dautova et al., 2019). Dense communities of octocorals have been reported on ridges of the seamount (Dautova et al., 2019) and Baco et al. (2017) also observed reef-forming scleractinians. Based on trawl surveys, the southern portion of Koko exhibits higher biodiversity than northern sites (Miyamoto et al., 2017). One explanation of this increased biodiversity could come from the habitat heterogeneity hypothesis, i.e. increased habitat heterogeneity leads to an increase in ecological niche space and therefore increased biodiversity (MacArthur and MacArthur, 1961). The HESC seamounts often exhibit heterogeneous environments on separate sides and between different depth bands of seamounts that are correlated, within a seamount, to changes in community structure and biodiversity (regional examples: Long and Baco, 2014; Mejía-Mercado et al., 2019; Mejía-Mercado and Baco, 2022, 2023, Morgan et al., 2015, 2019; Schlacher et al., 2014).

An alternative explanation for the observed community heterogeneity on Koko, however, could be that fishing effort varies by location on Koko. Historical fishing disturbance may be spatially or temporally distinct, leading to varied disturbance impacts and recovery across the seamount. Current fishing effort and persistent evidence of trawling such as trawl scars are tools that can track the extent and effects of current and historical fishing practices. Based on the Automatic Identification System (AIS) vessel behavior, Morgan and Baco (2020) observed greater coverage of expected trawling and fishing effort, in hours fished, on the northern portion of the seamount than the southern portion. Knowing that trawling homogenizes substrate and epibenthic communities, resulting in lower richness and evenness (Clark et al., 2016; Cryer et al., 2002; Koslow et al., 2001), one would expect greater disturbance in regions of higher fishing effort. The higher biodiversity on southern sites on Koko observed by Miyamoto et al. (2017), could therefore be the result of different levels of fishing effort and the subsequent varied fishing impacts to the communities. Varied fishing impacts could lead to a mosaic of remnant, recovering, and disturbed communities.

Koko is one site, within the most recent study of recovery on HESC seamounts, with evidence of both disturbed communities and potentially recovering populations (Baco et al., 2020, 2023a). Replicate submersible transects showed that the mean abundance of coralliids was generally lower on actively trawled sites than on never trawled sites, but at 500 m depth there was greater abundance on Koko (Baco et al., 2023a). The height and width of the corals on Koko were smaller than on never trawled sites which supports the process of recovery through new recruitment (discussed in Baco et al., 2023a). However, due to such early fishing effort, other than the precious corals (Baco et al., 2023a), there is little information on the baseline community and biodiversity of Koko prior to fishing effort. Therefore, a finer-scale analysis is required to assess the distribution and prevalence of benthic communities on Koko.

Thus, this study investigates the habitat and community heterogeneity on the heavily fished seamount, Koko Guyot, by characterizing both megafauna presence and evidence of fishing at a finer scale than previously investigated on the fished seamount. Fine-scale analyses investigate seamount megafauna and evidence of disturbance within multiple small sites on a single seamount rather than a broadscale analysis across the entire seamount or multiple seamounts. Previous studies included a subset of the surveys on Koko as a part of broad-scale analyses (Baco et al., 2019, 2020, 2023a). Autonomous Underwater Vehicle (AUV) imagery previously identified small areas of high abundance but were unable to identify taxa to family groups due to the vehicle height above the seafloor and the downward angle of the camera (Baco et al., 2019, 2020). Here, human occupied vehicles (HOVs) were used for surveys closer to the seafloor, with a camera that allowed a face-on view of the corals and megafauna, allowing for taxonomic identification to the species level. Multiple transects at two sites on the north and south sides of the southeast corner of Koko were analyzed to investigate 1) the composition, abundance, diversity, and ecosystem function of benthic megafaunal assemblages at each side and depth and 2) the anthropogenic and abiotic environmental factors potentially influencing assemblages at these sites.

2. Methods

2.1. Site

The HESC contains the Emperor Seamount Chain and the seamounts of the Hawaiian Ridge. Koko Guyot, at 35°15′N, 171°35′E, is the largest seamount within the HESC, with a summit area of 5800 km^2 (Clague et al., 1980). The carbonate capped guyot is over 50 million years old (Sharp and Clague, 1979) and has subsided to a summit depth of 260 m (Davies et al., 1972). There is evidence that the shallow tropical coral reef atop Koko stopped growing about 33 Ma as the guyot subsided (Clague et al., 2010). Few studies have investigated the geomorphology or water chemistry of Koko. However, seamount-associated eddies along the eastern side of Koko, as well as on Ojin/Jingu were observed using

drifters in the 1990s (Vastano et al., 1985; Bograd et al., 1997). As Koko is so large, only a small portion of the southeastern corner was explored here (Fig. 1).

2.2. Imagery surveys

Imagery was collected as part of a larger project to examine the effects of trawling disturbance on seamount benthic communities in the HESC (Baco et al., 2019, 2020, 2023a). In 2016 and 2017, the research vessel *Ka'imikai-O-Kanaloa* (KOK) was used to deploy the *Pisces IV* and *Pisces V* HOVs. The HOVs worked in tandem to survey three replicate 500 m long transects at depths of 400, 500, and 600 m at Northeast (NE) and Southeast (SE) sites on the southeastern corner of Koko, totaling 18 transects (Table 1, Fig. 1). "Site" is from this point used to refer to the

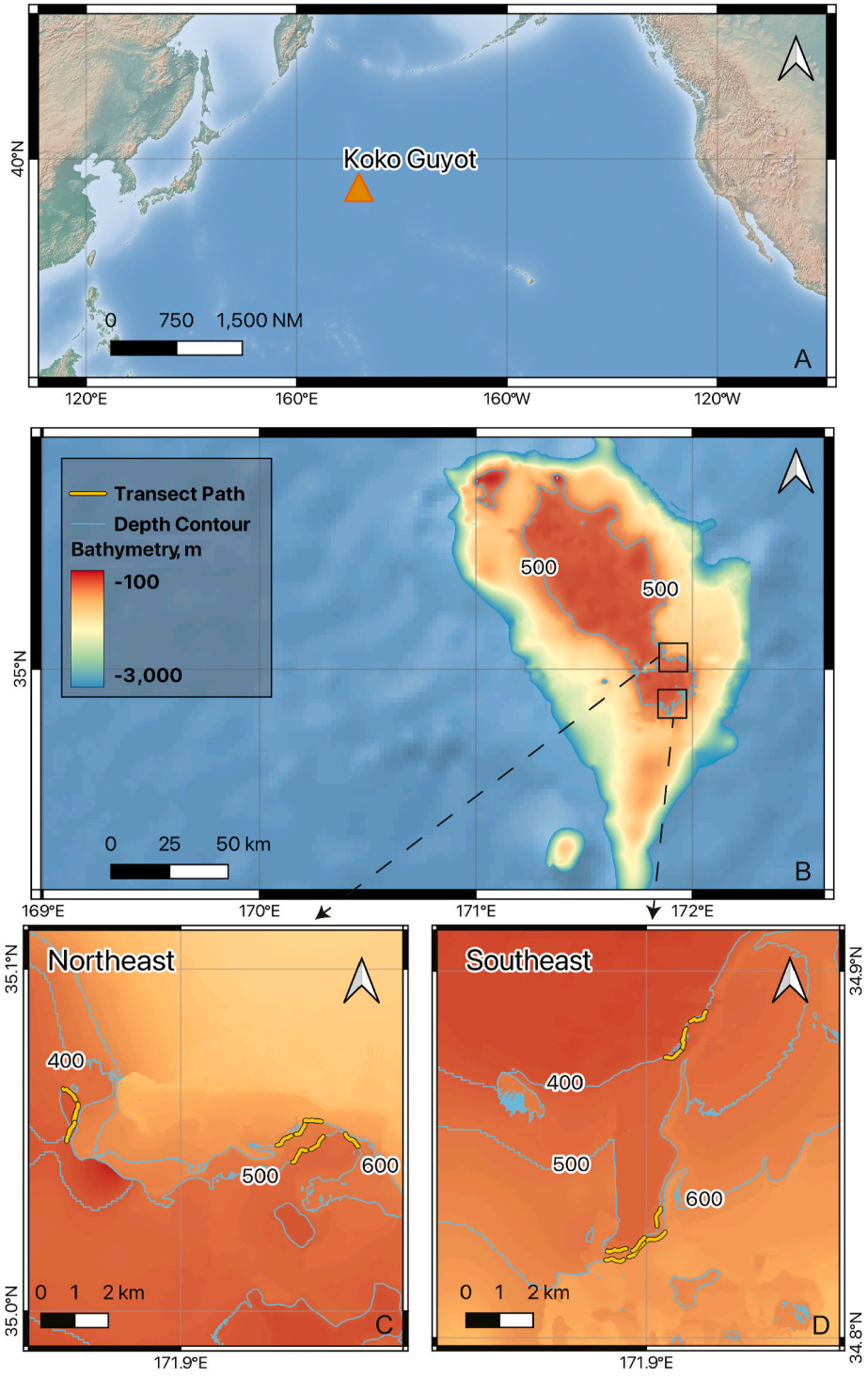

Fig. 1. Site map of the overall location within the Pacific Basin (A), Bathymetry of Koko of the Hawaiian- Emperor Seamount Chain (B) and the Northeast (C) and Southeast (D) study sites. The legend for maps B, C, and D is within B, highlighting the bathymetry of Koko with shallower sites red and deeper sites yellow. Gold lines represent the transect locations at 400, 500, and 600 m depths. Maps were created in QGIS v 3.36 using a resampled GEBCO 2021 bathymetry grid (GEBCO Bathymetric Compilation Group, 2021) and Natural Earth free raster layers from naturalearthdata.com. (For interpretation of the references to colour in this figure legend, the reader is referred to the Web version of this article.)

Table 1
Metadata for each annotated transect at 400, 500, and 600 m on the Northeast (NE) and Southeast (SE) Koko Guyot study sites, as well as the start position (in Degree Decimal Minutes) and total annotated length of each transect.

Date	Dive	Submersible	Depth, m	Side	Transect	Latitude, N	Longitude, E	Total length, m
9/21/17	893	*Pisces V*	400	NE	1	35 03.895	171 51.539	600
9/21/17	893	*Pisces V*	400	NE	2	35 03.625	171 51.839	700
9/21/17	893	*Pisces V*	400	NE	3	35 03.304	171 51.760	830
9/24/17	896	*Pisces V*	400	SE	1	34 53.337	171 55.159	680
9/24/17	896	*Pisces V*	400	SE	2	34 53.052	171 54.790	720
9/24/17	896	*Pisces V*	400	SE	3	34 52.732	171 54.690	650
9/20/17	325	*Pisces IV*	500	NE	1	35 02.898	171 57.712	640
9/22/17	327	*Pisces IV*	500	NE	1	35 03.058	171 56.982	620
9/22/17	327	*Pisces IV*	500	NE	2	35 02.822	171 56.633	730
9/23/17	328	*Pisces IV*	500	SE	1	34 49.418	171 53.230	630
9/23/17	328	*Pisces IV*	500	SE	2	34 49.448	171 53.690	610
9/23/17	328	*Pisces IV*	500	SE	3	34 49.795	171 54.216	630
9/22/17	894	*Pisces V*	600	NE	1	35 03.329	171 56.944	600
9/22/17	894	*Pisces V*	600	NE	2	35 03.319	171 56.602	630
9/22/17	894	*Pisces V*	600	NE	3	35 03.071	171 56.311	650
9/23/17	895	*Pisces V*	600	SE	1	34 49.274	171 53.196	600
9/23/17	895	*Pisces V*	600	SE	2	34 49.331	171 53.668	640
9/23/17	895	*Pisces V*	600	SE	3	34 49.597	171 54.019	640

side and depth combinations of each set of transects, e.g., 400 m SE. Between transects, specimens and imagery were collected for taxonomic identification and verification. Both HOVs had an Insite Pacific MINI-ZEUS HDTV camera on a pan and tilt system that were used to collect all imagery. Both vehicles followed an identical transecting protocol to ensure consistency: lights on, camera angle facing the substrate (remaining fixed throughout a transect) and maintaining a consistent altitude (about 1 m) and speed (about 0.5 knots). All transects started from a recorded position before traveling 500 m, then the vehicle stopped in a suitable location to record the final position. Transects were annotated from the recorded position when the vehicle was leaving the substrate to when the vehicle returned to the substrate with documented positions reported from the KOK using USBL sonar tracking.

2.3. Imagery annotations

Annotations for substrate type, substrate size, image roughness, and image slope followed standardized methods using still images (e.g., Long and Baco, 2014; Mejía-Mercado et al., 2019; Mejía-Mercado and Baco, 2022, 2023, Morgan et al., 2015, 2019). For substrate variables, single video frames were captured from the videos at 10 s intervals to eliminate overlap. ImageJ v1.51 (Schneider et al., 2012) was used to generate 15 random points on each image. These 15 points were annotated for substrate size and type. The categories of substrate type included basalt, carbonate, living biology, coral rubble, white sand, gray sand, and anthropogenic litter. Substrate sizes followed the Wentworth scale, including hardpan, pebble, cobble, and boulder, as well as coral rubble (Wentworth, 1922). As each image within a transect was annotated for substrate size and type using 15 points, the total number of annotations was 15 times the total number of images per transect. Total percent composition was then calculated for both substrate type and substrate size by dividing the number of annotations within a substrate category per transect by the total number of substrate annotations within a transect. This was calculated for each category of substrate size and substrate type. Image roughness and slope were assessed across the entire image using scales determined visually from low to high. Therefore, an average slope (1–4 for low slope to high slope) and average image roughness (1–5 for low roughness to high roughness) could be calculated across all images within a transect resulting in image slope and image roughness per transect (further characterization of the categories can be found in Supplemental Table 1).

Videos were annotated for benthic megafauna along a consistent 950-pixel width of the field of view consisting of the best lit portion of the imagery, to minimize bias from non-uniform illumination (similar to Morris et al., 2014). Transects were annotated in random order by a single annotator. Taxonomic identification followed established methodology in the HESC (Morgan et al., 2015, 2019). Each megafaunal individual observed was assigned a provisional identification to the lowest taxonomic resolution and assigned a confidence value on a scale from 1, being highest confidence, to 4 being lowest confidence (following Morgan et al., 2015, 2019). All confidence level observations were included for standardized abundance analyses. Only identifications of a score of 1 were included for diversity, multivariate, and trait analyses.

Observations of anthropogenic influence were annotated from the HOV imagery as part of the same annotation process as the benthic megafauna. Each observation of an anthropogenic object was annotated for material type and fishing or non-fishing origins. All observations of fishing and non-fishing materials were summed per transect into the metric, “Total Debris Abundance”. Total Debris Abundance includes all fishing gear, litter, and debris, e.g., soda cans, plastic bags, lines, and nets. Additionally, observations of trawl scars, visible scars on the seafloor where bottom-contact gear has marked the substrate, were counted per transect. All fishing material as well as observations of trawl scars were summed to create the joint metric of “Visual Evidence of Fishing”. Visual Evidence of Fishing does not include debris items that could have fallen from vessels other than fishing vessels, i.e., soda cans and plastic bags are not included in Visual Evidence of Fishing. Both Total Debris Abundance and the Visual Evidence of Fishing metrics were then standardized by transect length for analyses.

2.4. Environmental data collection

Table 2 contains an overview of the environmental parameters included in this analysis. Bathymetry, collected by an EM 122 Kongsberg multibeam echosounder aboard the *R/V Kilo Moana* in 2015, was used to derive the depth, slope, curvature, aspect, and topographic roughness index along each transect in QGIS v 3.22. ArcMap v10.4.1 was used to calculate bathymetric position index (BPI) finescale (3 and 25 inner and outer radii) and BPI broadscale (25 and 250 inner and outer radii). R v4.0.1.3 (R Core Team, 2022) was used to wrangle environmental data and for statistical analyses. R packages *ncdf4* v3.1-157 (Pierce, 2025) and *httr* v1.4.3 (Wickham, 2023), were used to download and manipulate netcdf files of the environmental parameters from the NOAA Environmental Research Division Data Access Program, ERDDAP (Wilson

Table 2
Environmental parameters utilized in the study. Bathymetry is from EM302 Kongsberg multibeam echosounder aboard *R/V Kilo Moana* in 2015 surveys.

Parameter Name	Units	Resolution	Source
Chlorophyll	mg m-3	0.025 deg	NASA - Aqua Modis
Salinity	PSU	0.025 deg	NASA - Aqua Modis
Surface Temperature	C	0.025 deg	NASA - Aqua Modis
Modeled Water Temperature	C	0.025 deg	HYCOM
Modeled Salinity	PSU	0.025 deg	HYCOM
Modeled v	cm/s	0.025 deg	HYCOM
Modeled u	cm/s	0.025 deg	HYCOM
Modeled Surface Elevation	cm	0.025 deg	HYCOM
Depth	m	0.0001 deg	Derived from bathymetry
Slope	(0–90°)	0.0001 deg	Derived from bathymetry
Curvature		0.0001 deg	Derived from bathymetry
Aspect	(0–360°)	0.0001 deg	Derived from bathymetry
Topographic Roughness	m	0.0001 deg	Derived from bathymetry
BPI finescale		0.0001 deg	Derived from bathymetry
BPI broadscale		0.0001 deg	Derived from bathymetry
Substrate Type	%	0.005 deg	Annotated
Substrate Size	%	0.005 deg	Annotated
Image Roughness		0.005 deg	Annotated
Image Slope		0.005 deg	Annotated

et al., 2020), including Aqua-MODIS chlorophyll (NASA Goddard Space Flight Center), and the Hybrid Coordinate Ocean Model (HYCOM, hycom.org (Chassignet et al., 2007)). Satellite and modeled environmental parameters include 10-year average surface chlorophyll, surface salinity, surface temperature, modeled water temperature, modeled salinity, modeled north-south current (v), modeled east-west current (u), and modeled surface elevation. The downloaded parameters were converted to rasters with a resolution of 0.025° using bilinear resampling, and values were extracted using R package *raster* v3.5-21 (Hijmans, 2025). Several additional Global Ocean Data Analysis Project (GLODAP v 2021 (Lauvset et al., 2021)) and Lamont-Doherty Earth Observatory Surface Ocean CO_2 Climatology parameters (Takahashi et al., 2014) were initially included in the analysis but due to the proximity of the sites and transects (16 km between sites, and ~100 m between transects) and the low resolution of the data, there was no variation among transects on a single side. Although initially included, due to lack of variability across the area of study, these parameters were also excluded from multivariate analyses; oxygen, nutrients, temperature at 600 m, total organic carbon, anthropogenic carbon, total alkalinity, pH, aragonite saturation state, and calcite saturation state.

2.5. Statistical analysis

2.5.1. Univariate data and analyses

Abundance within a transect was totaled for the faunal observations for all confidence values in the dataset and standardized by dividing by the total transect length for each transect. Diversity and multivariate analyses used only annotations with a taxonomic confidence level of 1. Hill diversity indices for species richness ($\alpha = 0$), Shannon Entropy ($\alpha = 1$), and inverse Simpson's Dominance ($\alpha = 2$), up to the Berger-Parker dominance ($\alpha = \infty$), were calculated for each transect (Hill, 1973; Chao et al., 2014). A Rényi plot was used to visualize the difference in diversity between sites (Rényi, 1961; Tóthmérész, 1995). As Rényi's diversity index is the natural log of Hill's diversity index, this plot can be used to visualize the diversity calculated here while also providing measures of diversity along the gradient of influence of dominant taxa (Rényi, 1961; Tóthmérész, 1995). As α increases, the influence of the dominant taxa increases, from species richness where all taxa are equal to the inverse Berger-Parker dominance which calculates the abundance of only the most dominant taxa. These diversity indices and total abundance were tested for normality using the Shapiro-Wilk test (Shapiro and Wilk, 1965). Hill diversity metrics were found to be normally distributed while standardized total abundance, Total Debris Abundance, and Visual Evidence of Fishing were not normally distributed. A two-way crossed analysis of variance (ANOVA) was run with depth and side as fixed factors for all indices as it has been shown that ANOVA is robust to non-normally distributed data (Feir-Walsh and Toothaker, 1974; Blanca et al., 2017, 2023). The results of the ANOVA were plotted on QQ plots to assess the fit. Packages used in R for these univariate tests include *hillR* v0.5.1 (Li, 2018) for Hill diversity indices, and base R v4.1.3 (R Core Team, 2022) for Shapiro-Wilks and ANOVA.

To understand the potential influence of historical fishing and derelict fishing gear on megafauna communities on Koko the relationships between both total megafaunal abundance and species richness with Visual Evidence of Fishing were investigated using a linear regression.

2.5.2. Multivariate data and analyses

Multivariate analyses used the package *vegan* (Oksanen et al., 2019) in R or the statistical software Primer v7.0.13 (Anderson et al., 2008). To test for variance in community structure, a PERMANOVA was used with depth and side as factors. The community structure was visualized using a nMDS plot of the square-root transformed Bray-Curtis dissimilarity matrix.

Distance based linear modeling (DistLM) was used to determine the environmental parameters that best explained the variance in the dataset using PRIMER (Anderson et al., 2008). Environmental variables were filtered prior to analyses. Parameters tested for inclusion in the dbRDA analysis include those in Table 2, as well as the annotated metrics of Total Debris Abundance, Visual Evidence of Fishing, and abundance of trawl scars as metrics of potential anthropogenic influence and fishing effort. Spearman correlation was used to remove correlated variables from the dataset. Variance inflation factor (VIF) was used to further filter correlated variables until all VIF values were less than 10. The final parameters included: 10-year mean chlorophyll, percent sand, bathymetry derived aspect, bathymetry derived slope, bathymetry derived curvature, bathymetry derived BPI finescale and broadscale, Visual Evidence of Fishing, and presence of trawl scars. AIC was used to calculate the best model. Results were plotted on the first two dbRDA axes in R using *vegan* v2.6.8 (Oksanen et al., 2019).

2.5.3. Indicator species

Using the R package *indicspecies* 1.7.12 (De Cáceres and Legendre, 2009), the individual taxa that were most associated with each site were determined (De Cáceres et al., 2010). These results were filtered to statistically significant interactions, p-value < 0.05.

2.6. Trait analysis

Functional traits, in this case morphological and ecological traits, were used to assess the ecological role of species within their community. Here four functional trait classes were assessed to test for potential effects of fishing disturbance on ecosystem function: Individual Colony Structure, Group Colony Structure, Trophic Guild, and Mobility. The first two of these were morphological traits related to the ability of a species to form habitat: Individual Colony Structure and Group Colony Structure. Individual Colony Structure forming taxa were primarily sponges, most gorgonians, and several scleractinians. Group Colony Structure includes those taxa known to create three-dimensional structure among multiple colonies in the form of coral reefs, coral gardens or forests, as well as sponge beds. A third trait class was Trophic Guild, differentiated into suspension feeders and non-suspension feeders, the latter including predators and scavengers. The final trait class, Mobility,

included two categories: sessile and mobile. Community trait proportions were then calculated across transects for number of species and overall abundance. Proportional trait species richness was calculated per trait by dividing the number of species within a transect with each trait by the total number of species within the transect. Whereas proportional trait abundance was calculated per trait by dividing the number of fauna observations within a transect with each trait by the total number of fauna annotations within the transect. Proportional abundance of each of the four sets of community functional traits were then regressed on Visual Evidence of Fishing.

3. Results

3.1. Substrate

Hardpan carbonate was the dominant substrate type (average: 91 %, range: 33–100 % of a transect) observed across all 18 transects conducted on Koko Guyot. Few boulders, cobbles or pebbles and little coral rubble were observed. Less than two percent coral rubble was found within the 500 m and 600 m zones, and no coral rubble was observed at the 400 m depth zones on either side. Sand was less than 10 % of the substrate composition per transect, except one transect on the NE side at 600 m depth that was 60 % sand. Image derived and bathymetry derived

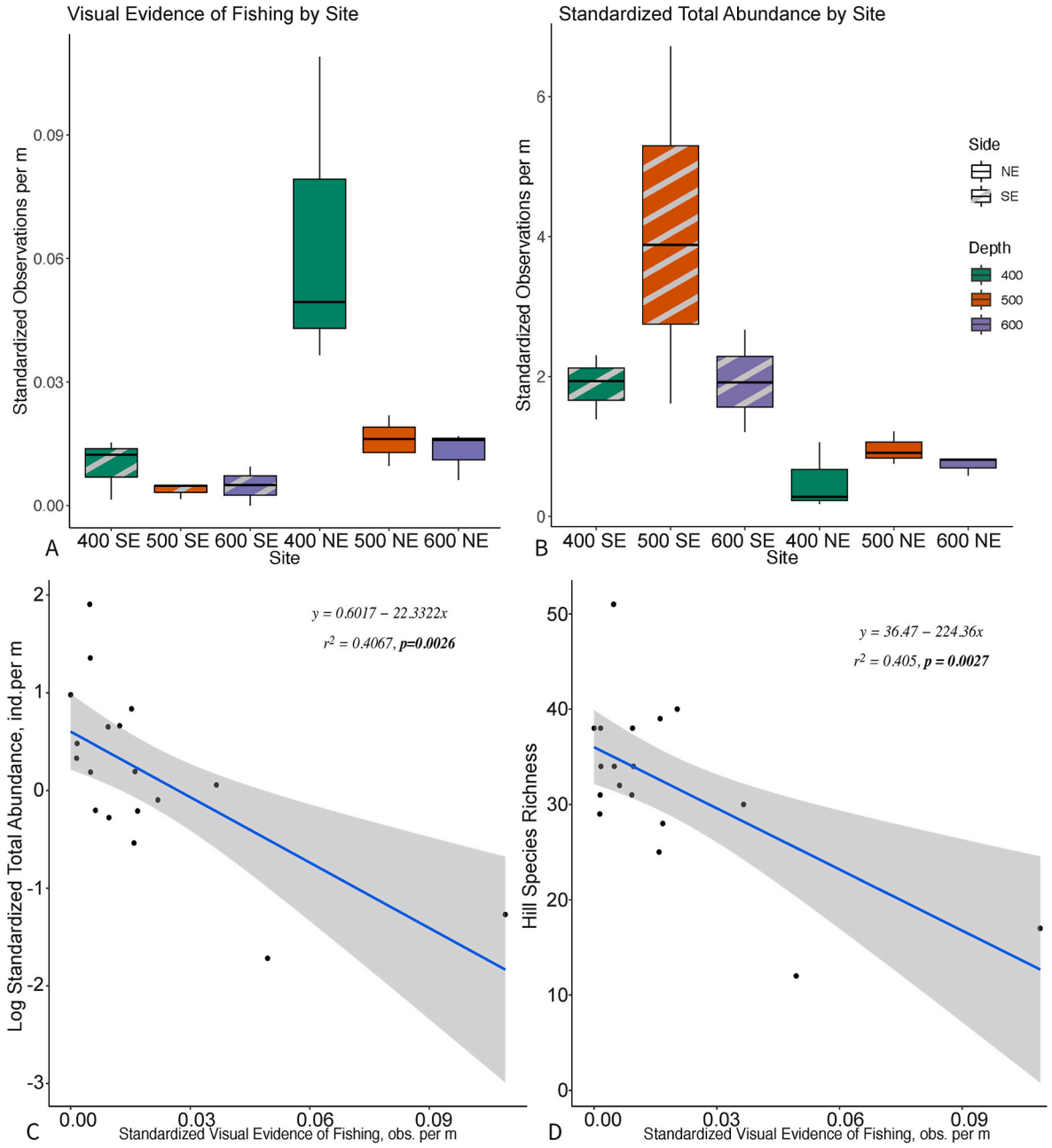

Fig. 2. (A) Boxplot representing the standardized Visual Evidence of Fishing observed at each site. Visual Evidence of Fishing incorporates derelict fishing gear and the abundance of trawl scars. (B) Boxplot representing the standardized total abundance of fauna observations per site. Colors note the depth zone, while filled boxes with no lines represent the NE sites and boxes containing gray diagonal lines represent the SE sites. (C) Regression of the log standardized total abundance per transect against Standardized Visual Evidence of Fishing, with regression line and equation, and (D) Regression of Hill's Species Richness against Visual Evidence of Fishing, with regression line and equation. Points represent transects in the regression plots, gray shadow denotes the 95 % confidence interval. Bolded numbers indicate p-value <0.05. (For interpretation of the references to colour in this figure legend, the reader is referred to the Web version of this article.)

slope and roughness were similar between transects, with the greatest bathymetry derived slope observed on the deepest transects at 600 m, and the greatest bathymetry derived topographic roughness observed at the 500 m SE sites. There was a pattern of decreasing BPI with increasing depth for both fine scale and broadscale BPI (Supplemental Fig. 1).

3.2. Debris observations and abundance

Debris and derelict fishing gear were observed at every site, with a total of 236 anthropogenic debris items observed, averaging 0.2 per m overall. Total Debris Abundance included glass bottles, fishing weights and lines, plastic, rubber buoys, and netting. A total of 20 sets of trawl scars were observed on the seafloor; included within Visual Evidence of Fishing (Fig. 2A, Supplemental Fig. 2). Overall, the dominant debris types were nets and lines found at all sites. The NE sites had a greater composition of net observations than the SE sites (Supplemental Fig. 2), while two of the SE sites had a greater proportion of trawl scars. The mean Visual Evidence of Fishing was greater on NE sites than the SE sites at all depths (Fig. 2A). Greatest Visual Evidence of Fishing was found at the 400 m NE sites, similar to overall debris.

When tested against the null hypothesis of no change between sites, Total Debris Abundance differed significantly overall ($p = 0.0028$, $F = 6.3$, $df = 5$) by depth ($p = 0.0221$, $F = 8.571$, $df = 2$) by side ($p = 0.0032$, $F = 9.151$, $df = 1$) and the interaction of side and depth ($p = 0.0203$, $F = 5.505$, $df = 1$) (Table 3). Visual Evidence of Fishing also varied between sites overall ($p = 0.0057$, $F = 5.8657$, $df = 5$), by depth ($p = 0.0180$, $F = 5.7156$, $df = 2$), by side ($p = 0.0073$, $F = 10.4142$, $df = 1$), and the interaction of depth and side ($p = 0.05$, $F = 3.7417$, $df = 2$) (Table 3).

3.3. Benthic megafaunal observations and abundance

Over 18,700 faunal observations were annotated in this study. Megafauna included scleractinian corals (e.g., *Enallopsammia rostrata* and *Madrepora oculata*), octocorals (e.g. *H. laauense* and *Chrysogorgia geniculata*), and antipatharians, as well as Hexactinellid sponges, echinoderms (e.g. Brisingid sea stars and Gorgonocephalidae basket stars), and crustaceans (e.g., the purple *Chaceon imperialis)*. Scleractinians observed included solitary cup corals, colonial fan morphotypes, and patches of reef-forming colonies. Precious red corals were observed at several sites, although not on all transects on Koko in this study. While not annotated, a surprising number of small sharks were observed on Koko as well (Supplemental Fig. 3).

Corals were by far the dominant group on the surveyed areas of Koko. Octocorals (Octocorallia and *Acanthogorgia* spp.*)* comprised over 60 % of the overall abundance (Fig. 3A). Multiple sites were dominated by yellow Paramuriceids in the genus *Acanthogorgia* to the point that they comprised 24 % of the overall composition across sites. Almost 20 % of the community on Koko were scleractinian corals. Distinct colonies of reef forming scleractinians on Koko include pink, orange, and white varieties often observed in small clumps. Both *M. oculata* and *Solenosmilia variabilis* are present on Koko (Miyamoto et al., 2017), however HOV imagery is unreliable for differentiating between the two, so they were annotated as a single morphotype. While no reef structures were observed on Koko in this study, *M. oculata* and *S. variabilis* form reefs at other features within the HESC (Baco et al., 2017). Of the scleractinians observed overall, 15 % were reef forming and 85 % were non-reef forming species (Fig. 3B). The next most abundant higher taxonomic group was Porifera with 8 % of the overall abundance, and the remaining other invertebrates composed 5 % of the assemblages and included crustaceans and echinoderms. Antipatharians comprised less than 2 % of the total Koko composition.

Similar to the overall assemblage, the most prevalent taxon at each site were types of corals, predominantly octocorals (Fig. 3A). Dominant octocorals include the distinct yellow *Acanthogorgia* spp. with almost 50 % of the observations at the 400 m NE site. This taxon was also the most abundant single octocoral group at the 500 m SE site, making up 12 % of the composition. An antipatharian whip coral was also an abundant coral with their greatest numbers at the 500 m NE site. These whip corals were not observed at the 600 m sites. Both 600 m NE and 500 m NE sites were dominated by scleractinians, which were almost entirely cup corals. The greatest proportion of reef-forming scleractinian species was observed at the 500 m SE transects (Fig. 3B). Increasing in percent composition with depth, scleractinians were more prevalent at the NE sites in comparison to the SE sites, comprising more than 65 % and 50 % total composition of the 600 m NE and 500 m sites, respectively, but at all other sites were <10 % (Fig. 3A). Sponges comprised 17 % of the total community at the 600 m SE site, but at all other sites sponges comprised less than 10 % of the total assemblage. Example images of communities observed in the 400 m NE and 500 m NE sites in comparison to the 500 m SE sites are included in Fig. 4.

A species of note due to the historical fishing pressure of this target species, the precious red coral *H. laauense,* was rarely observed on Koko. The greatest number of observations of this coral were made on the SE sites overall, with a total of 0.35 observations per m on SE sites and 0.18 observations per m on NE sites. The greatest number of coralliids observed was at the 500 m SE site followed by the 500 m NE site (0.27, 0.12 individuals per m respectively). Overall, 400 m and 600 m had only 0.04 observations per m and 0.10 observations per m respectively.

The 500 m depth zone transects on the SE site had the greatest total megafauna abundance within the study, with one transect totaling more than 4000 observations overall (Fig. 2B). The lowest abundance was found at the 400 m depth zone transects on the NE side. Standardized total abundance was greater on SE transects than NE, often double the mean abundance found on the NE transects at the same depths (Fig. 2B). Standardized total megafaunal abundance varied significantly overall ($p = 0.0212$, $F = 4.0905$, $df = 5$) and by side ($p = 0.0038$, $F = 12.7557$, $df = 1$). While abundance was generally greater at 500 m than the 400 m or 600 m transects, neither the difference in abundance with depth nor the interaction of depth and side were significant (Table 3).

Anthropogenic factors were further investigated by plotting the Visual Evidence of Fishing against the log standardized total megafauna abundance and species richness (Fig. 2C and D). There was a pattern of decreasing abundance and number of species with increased Visual Evidence of Fishing (Abundance: $R^2 = 0.4067$, $p = 0.0026$; Species Richness: $R^2 = 0.0405$, $p = 0.0027$).

3.4. Diversity

The Rényi diversity index, Fig. 5, highlights the change in diversity, with the influence of dominant taxa on the diversity index increasing as α increases. The Rényi index is directly related to the common Hill diversity indices which makes it ideal for visualizing diversity (Tóthmérész, 1995). As reviewed by Tóthmérész (1995), when comparing sites using a Rényi plot one can assume the greater diversity is at a site that is wholly above other lines on the plot and does not cross paths with the line of another site. Evidence of this is seen in Fig. 5, with the 500 m NE site being wholly above the 400 m NE and SE line as well as the 600 m NE line. This suggests that the 500 m NE site has greater overall diversity than 400 m NE, 400 m SE, and 600 m NE. Additionally, the 600 m SE Rényi index line is greater than the 400 m SE line, indicating 600 m SE has greater overall diversity than 400 m SE. However,

Table 3
Results of a two-way ANOVA with depth (400, 500, or 600 m) and side (NE or SE) as factors. Bolded values indicate p-value <0.05.

Metric	Overall	Depth, m	Side	Interaction
Total Debris Abundance	**0.0028**	**0.0221**	**0.0032**	**0.0203**
Visual Evidence of Fishing	**0.0057**	**0.018**	**0.0073**	0.05
Total Abundance	**0.0212**	0.1226	**0.0038**	0.2994
Species Richness	**0.0069**	**0.0034**	**0.0169**	0.54
Shannon's Entropy	**0.0334**	0.0846	**0.0346**	0.0886
Inverse Simpson's Dominance	**0.0243**	0.1106	**0.024**	0.0522

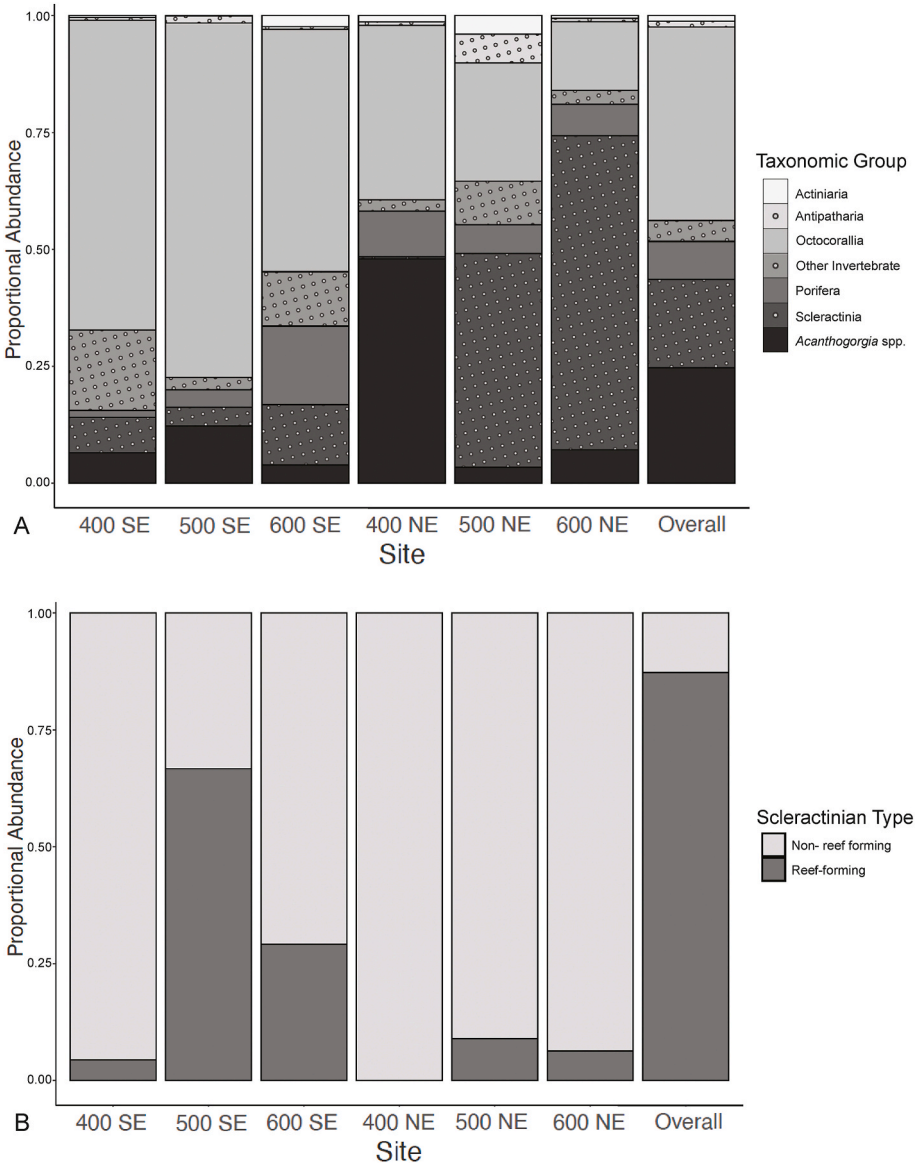

Fig. 3. (A) Proportional abundance of benthic megafaunal groups at each site and overall. (B) Proportional composition of reef-forming vs non-reef forming species at a site and overall.

the 500 m SE line crosses all others, so there can be no comparisons of overall diversity to this site, solely comparisons of the components of diversity: richness, Shannon Entropy, inverse Simpson's Dominance, and Berger-Parker dominance.

At an α of 0 all taxa are weighted equally to calculate species richness. All NE sites show lower species richness than the SE sites within the same depth zones (Fig. 5). The SE sites have lower Shannon Entropy than the NE sites at an α of 1. At 400 m and 500 m, the divergence of diversity patterns between NE and SE sites becomes more apparent with increasing influence of dominant taxa. As α increases to 2, inverse Simpson's Dominance, the SE sites decrease in evenness, leading to lower values of inverse dominance, while the NE sites have greater values of inverse dominance (increased evenness) than the SE sites at 400 m and 500 m. The 600 m transects are more similar in dominance between respective NE and SE sites. The last points at ∞, represents the inverse Berger-Parker dominance, which is greatest on the NE sites at all depths, except at 600 m where the two sides are equal.

Interestingly, the 500 m SE site shows the lowest inverse Simpson's dominance (lowest evenness) and the highest richness, while 400 m NE site shows the lowest richness and 500 m NE has the greatest inverse dominance (Fig. 5). In the two-way ANOVA tests, all diversity metrics had significant overall tests (Table 3). The three diversity metrics also differed significantly by side (Richness: $p = 0.0169$, $F = 7.6866$, $df = 1$; Shannon's Entropy: $p = 0.0346$, $F = 5.6738$, $df = 1$; Inverse Simpson's Dominance: $p = 0.024$, $F = 6.6678$, $df = 1$) but no index differed significantly by the interaction of side and depth (Table 3). Richness was the only single index which differed significantly by depth ($p = 0.0034$, $F = 9.5051$, $df = 2$) (Table 3).

3.5. Multivariate statistics

Based on PERMANOVA, the assemblage structure differed significantly across all sites, (overall $p = 0.001$, $F = 5.7275$). Assemblage structure differed between sides (side: $p = 0.003$, $F = 4.1868$), between depths (depth: $p = 0.002$, $F = 9.1603$), and with the interaction of depth and side (depth: side $p = 0.001$, $F = 3.0650$). The variation in community structure, as shown in the nMDS plot in Supplemental Fig. 4, organizes the communities on Koko by depth along the x-axis with all NE sites also separated above the SE sites on the y-axis (non-metric fit $R^2 = 0.995$, stress = 0.073). The transects at 400 m depth have the greatest

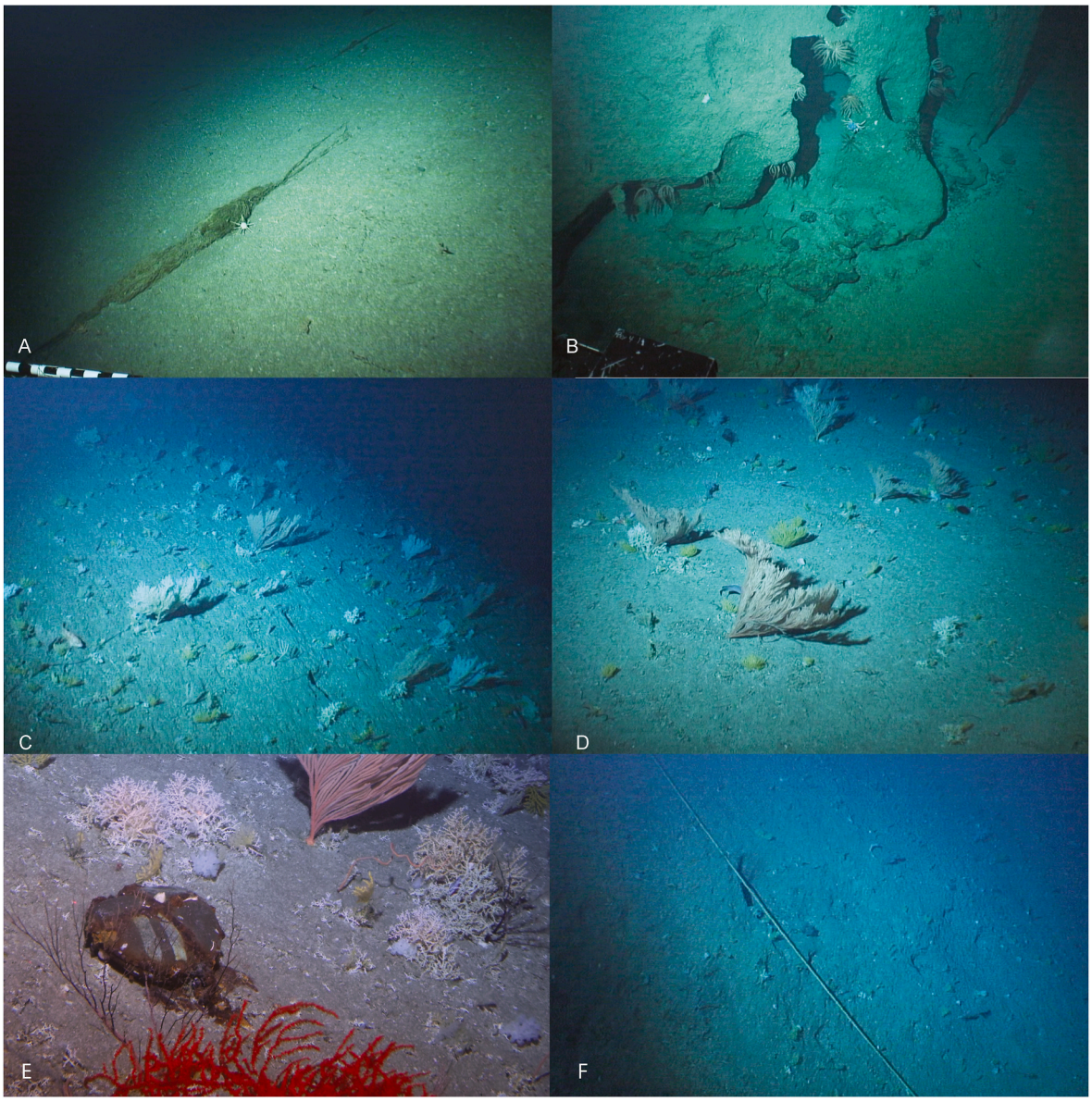

Fig. 4. Example images of benthic megafauna communities found on Koko Guyot. (A) Cidaroid urchin near netting on 400 m NE. (B) Brisingids and a purple *Chaceon imperialis* crab hanging from the cliff face at 500 m NE site. (C & D) Diverse assemblage of corals at 500 m SE. Example derelict fishing gear items included within Visual Evidence of Fishing, (E) a weight with chain and (F) a thick line. (For interpretation of the references to colour in this figure legend, the reader is referred to the Web version of this article.)

dissimilarity between the NE and SE sites at the same depth, while the 600 m transects have the smallest dissimilarity.

3.6. Indicator taxa

A total of 21 taxa were indicated as significantly associated with one or more site (Table 4). The 400 m SE transects were highly associated with multiple primnoids, antipatharian whip corals, and a non-reef forming scleractinain. The 500 m SE site was highly associated with primnoids, the abundant yellow *Acanthogorgia* spp. as well as the structure forming coralliids. The SE site at 600 m was associated with a small white scleractinian and a reef-forming scleractinian species. A cidaroid urchin was the only taxon associated with the 400 m NE transects. The 500 m NE cluster was most associated with two medium sized primnoid taxa and a brisingid. The 600 m NE cluster was associated with small sea urchins, a feathery brisingid, a small anemone, and a flexible *Chrysogorgia*.

3.7. Functional trait analysis

Visual Evidence of Fishing was significantly correlated with each of the categories of functional traits (Fig. 6). Increasing Visual Evidence of Fishing when modeled with Individual Colony Structure and Group Colony Structure showed a negative correlation with the proportion of traits by species (Fig. 6A and B; $r^2 = 0.6733$ $p < 0.0001$, $r^2 = 0.2092$ $p = 0.0323$) and a similarly negative, though less strong correlation with proportion of trait abundance (Supplemental Fig. 5A and B; $r^2 = 0.1871$ $p = 0.0415$, $r^2 = 0.0809$ $p = 0.1337$). Similarly, for Trophic Guild, the proportion of suspension feeders decreased with Visual Evidence of Fishing (Fig. 6C; $r^2 = 0.464$ $p = 0.0011$), with an increase in proportion of non-suspension feeders, predators and scavengers. This aligns with the results for the Mobility classes which indicated a decrease in sessile fauna with increasing Visual Evidence of Fishing (Fig. 6D, $r^2 = 0.1968$ $p = 0.0372$).

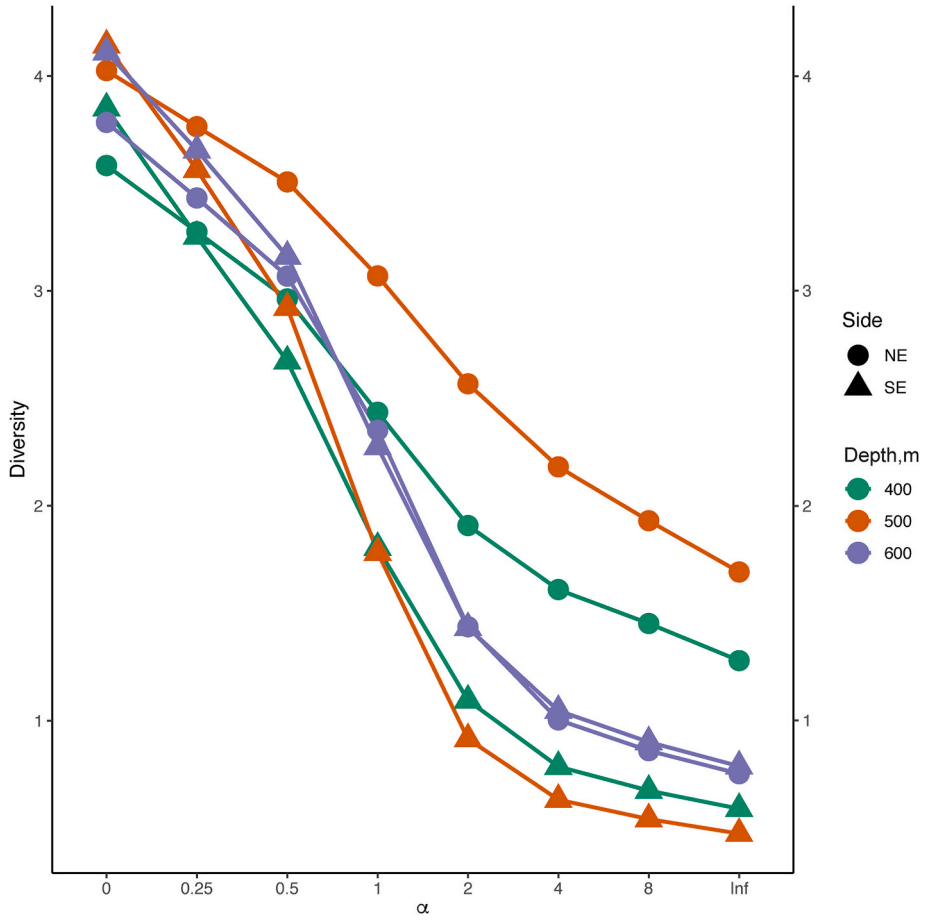

Fig. 5. Plot of the Rényi diversity index calculated for each site. The y axis is the value of the calculated diversity while the x axis is α which determines how abundance is weighted in the diversity calculation. As α increases from zero to infinity, the influence of dominance increases. An α of 0 is equivalent to species richness, an α of 1 is equivalent to Shannon's Entropy, an α of 2 is equivalent to inverse Simpson's Dominance (evenness), and an α of ∞ is equivalent to inverse Berger-Parker Dominance.

3.8. Environmental and anthropogenic factors

After removing correlated environmental and anthropogenic variables, nine parameters were left to include in the dbRDA analysis (Table 5A). The strongest correlates to the observed community structure individually (Table 5A) were Visual Evidence of Fishing ($p = 0.007$), Slope ($p = 0.001$), BPI broadscale ($p = 0.001$), and BPI finescale ($p = 0.052$), and each explained high proportions of the total variance (Visual Evidence of Fishing 0.1384, Slope 0.2084, BPI broadscale 0.1145, and BPI finescale 0.3212) (Table 5A). The best fit model included only three variables, Visual Evidence of Fishing, BPI finescale, and BPI broadscale (Table 5B). Although slope individually explained 21 % of the variance it reduced the fit when added back into the model. Visual Evidence of Fishing, BPI finescale, and BPI broadscale together explained 51.99 % of the total variation. Sites were clearly separated by depth along dbRDA axis 1 (Fig. 7), which was most strongly correlated with BPI broadscale (correlation of 0.995, Table 5C). Most SE transects within each depth group were observed above the NE site transects for each depth on dbRDA axis 2. This was most pronounced in the 400 m transects. This axis correlates most strongly with Visual Evidence of Fishing (correlation of 0.971, Table 5C). The 3rd axis (not plotted) was most strongly correlated with BPI finescale (correlation of −0.971, Table 5C).

4. Discussion

Seamount communities have been impacted by industrial bottom-contact fishing efforts for over half a century (reviewed in Clark et al., 2007), yet there is still little understanding of the scale of disturbance, or of the potential for ecosystem recovery or resilience to such disturbance. Individual seamounts are often treated as entirely impacted or entirely pristine, but there is evidence that fishing practices and fishing sites can change through time on a given feature (Morgan and Baco, 2020; Stelzenmüller et al., 2008). This could result in heterogeneous patterns of disturbance. Previous studies on Koko Guyot reflect this variability, with findings of a high diversity of coral taxa (Miyamoto et al., 2017; Dautova et al., 2019), patches of high faunal abundance in AUV imagery, as well as low abundance areas and evidence of bottom contact fishing (Baco et al., 2019, 2020). However, these studies did not provide a fine-scale analysis of faunal communities in relation to environmental or fishing impact data. Other similar studies used satellite fishing hours (Morgan and Baco, 2020), or fishing history of entire features (Baco et al., 2019, 2023a) in comparison to community metrics, whereas the current study investigates patterns of fishing evidence taken from the same imagery used for community metrics. After half a century of fishing, Koko still hosts a heterogeneous array of benthic fauna displaying a mosaic of communities spanning high abundance structure-forming sessile suspension feeding assemblages, to impacted sites with low abundance of predominantly higher mobility scavenging assemblages.

4.1. Observed debris patterns

Observations of derelict fishing gear on Koko were generally higher than has been documented at other fished seamounts or canyons

Table 4
Indicator species, here labeled by morphospecies number, that had significant values for each site with association statistic and significance. Bolded numbers indicate p-value <0.05.

Site	Taxa	Association	p-value	
400 NE				
	Urchin.03	0.98	0.02	*
400 SE				
	Scleractinia.10	1	**0.015**	*
	Primnoid.03	1	**0.015**	*
	Primnoid Unbranched	0.938	**0.025**	*
	Paramuriceid.02	0.881	**0.015**	*
	Paramuriceid.01	0.861	**0.035**	*
	Antipatharia.11	0.851	**0.015**	*
	Antipatharia.03	0.836	**0.04**	*
500 NE				
	Primnoid.01	0.911	**0.015**	*
	Brisingid.01	0.889	**0.01**	**
	Primnoid.12	0.668	**0.02**	*
500 SE				
	Yellow Acanthogorgia	0.972	**0.005**	**
	Primnoid.08	0.927	**0.005**	**
	Primnoid.10	0.858	**0.005**	**
	Coralliid	0.831	**0.005**	**
600 NE				
	Urchin.04	1	**0.005**	**
	Actiniaria.01	1	**0.005**	**
	Brisingid.03	0.977	**0.005**	**
	Chrysogorgia.01	0.776	**0.01**	**
600 SE				
	Scleractinia.01	0.942	**0.005**	**
	Scleractinia Pink	0.897	**0.005**	**

(reviewed in Amon et al., 2020), which would be consistent with known high fishing activity over multiple decades on Koko. Cobb Seamount, another North Pacific feature with an extensive fishing history, had an average of 7 items per km ranging up to 29 items per km (Du Preez et al., 2020), whereas on Koko, an average of 20 items per km were found, with one transect having 76 debris items within the 700 m transect (which extrapolates to 109 observations per km). Similarly, both Cobb Seamount and Koko showed variability in the spatial distribution of derelict fishing gear on the features. This could indicate seamounts of the Pacific, not just Koko, exhibit variability in fishing effort within a feature.

4.2. Overall community composition

Benthic assemblages on Koko were dominated by octocorals at each site, reflecting regional observations across the north and central Pacific (Long and Baco, 2014; Morgan et al., 2015, 2019; Auscavitch et al., 2020; Parrish, 2007; Parrish and Boland, 2004; Baco, 2007). However, antipatharians composed a smaller proportion of the overall assemblage on Koko (<2 %) compared to central Pacific seamounts (12 %) (Auscavitch et al., 2020). In the central North Pacific, deep-sea scleractinian reefs are relatively rare (Baco et al., 2023b), although they have been found on seamounts on the northwestern end of the HESC seamounts from Koko to Pioneer Bank (Baco et al., 2017, 2023b). Scleractinian colonies were found within all sites studied here except the site with the greatest Visual Evidence of Fishing (400 m NE). Although no reef structures were observed on the transects in this study, a significant percentage of the communities on Koko were comprised of colonies of scleractinian species known to form reefs.

The most abundant coral overall was the yellow octocoral *Acanthogorgia* spp. (Family Paramuriceidae). This genus has been found previously on Koko (Miyamoto et al., 2017; Dautova et al., 2019) and paramuriceids are found in abundance on central Pacific seamounts (Auscavitch et al., 2020). On the Makapu'u coral bed paramuriceids were the third most abundant family (Long and Baco, 2014) and paramuriceids were prominent on two sites on Mokumanamana (Morgan et al., 2019). However, the dominance found on Koko across sites is much greater (25 % of total composition) in comparison to these other studies. In contrast, the coralliid precious red coral, *H. laauense*, is found in high abundance on seamounts of the Hawaiian Ridge (Baco et al., 2023a; Long and Baco, 2014; Parrish, 2007; Baco, 2007) but in low abundance on Koko (0.6 % of total composition). This result for coralliids was expected, as a subset of these transects were included in a previous analysis across the HESC that showed a reduction in both size and abundance of coralliids at sites with a history of fishing (Baco et al., 2023a). The disproportional abundance of the *Acanthogorgia* spp. is harder to explain. Paramuriceid octocorals are relatively fast growing in comparison to other corals, including coralliids, with growth rates for *Paramuricea* spp. specimens of 0.56 ± 0.05 and 0.58 ± 0.08 cm/yr, determined by bomb radiocarbon dating (Sherwood and Edinger, 2009). Consequently, the observed dominance of this taxon across Koko could be explained given these comparatively rapid growth rates if this species is also capable of rapid colonization through fragmentation or high local recruitment. Overall, the prevalence of paramuriceids and the lack of coralliids is not consistent with the never trawled or protected recovering sites within the Papahānaumokuākea National Marine Sanctuary.

4.3. Abundance and diversity patterns

It is common for abundance, diversity, and community composition to vary with changing depth on seamounts (Long and Baco, 2014; Morgan et al., 2015; Victorero et al., 2018). Variation in abundance and diversity across depth bins and sides on Koko also reflect depth-related diversity gradients and horizontal gradients in diversity that have been observed on other HESC seamounts, (e.g., Mejía-Mercado et al., 2019; Mejía-Mercado and Baco, 2022, 2023; Morgan et al., 2019). For example, on the unfished HESC feature Mokumanamana, all diversity metrics also vary with both depth and seamount side (Morgan et al., 2019).

On Koko, the variation in abundance and diversity were also significantly correlated with Visual Evidence of Fishing. The statistically significant inverse relationship of Visual Evidence of Fishing to abundance and species richness found here has also been observed on actively trawled and recently fished seamounts in the South Pacific (Clark et al., 2019; Althaus et al., 2009). A subsequent study showed that those sites had not recovered in either abundance or diversity in the 15 years since the end of trawling (Clark et al., 2019). Similarly, the significant correlation of Visual Evidence of Fishing with megafaunal abundance on Koko likely reflects the persistent effects of fishing pressure. Even after fishing pressures are removed from a region, derelict fishing gear continues to negatively impact benthic seamount communities (Yoklavich et al., 2018; Gilman et al., 2021). Therefore, Visual Evidence of Fishing is not only evidence of fishing practices but also implies ongoing impacts to these sites.

4.4. Community structure patterns and drivers

Assemblage structure on Koko and other features within the HESC, including Mokumanamana Island and the Makapu'u coral bed, similarly show a separation of benthic assemblage structure by depth (Long and Baco, 2014; Morgan et al., 2019) and both Koko and Mokumanamana had variation in structure by side (Morgan et al., 2019) that are also reflected in benthic fishes of the HESC (Mejía-Mercado et al., 2019; Mejía-Mercado and Baco, 2022, 2023), highlighting the influence of habitat heterogeneity on seamount benthic communities. This pattern may be generalizable as it was also observed on the Graveyard features off Tasmania, with benthic faunal assemblage correlated to depth, but also to environmental parameters such as slope (Goode et al., 2021).

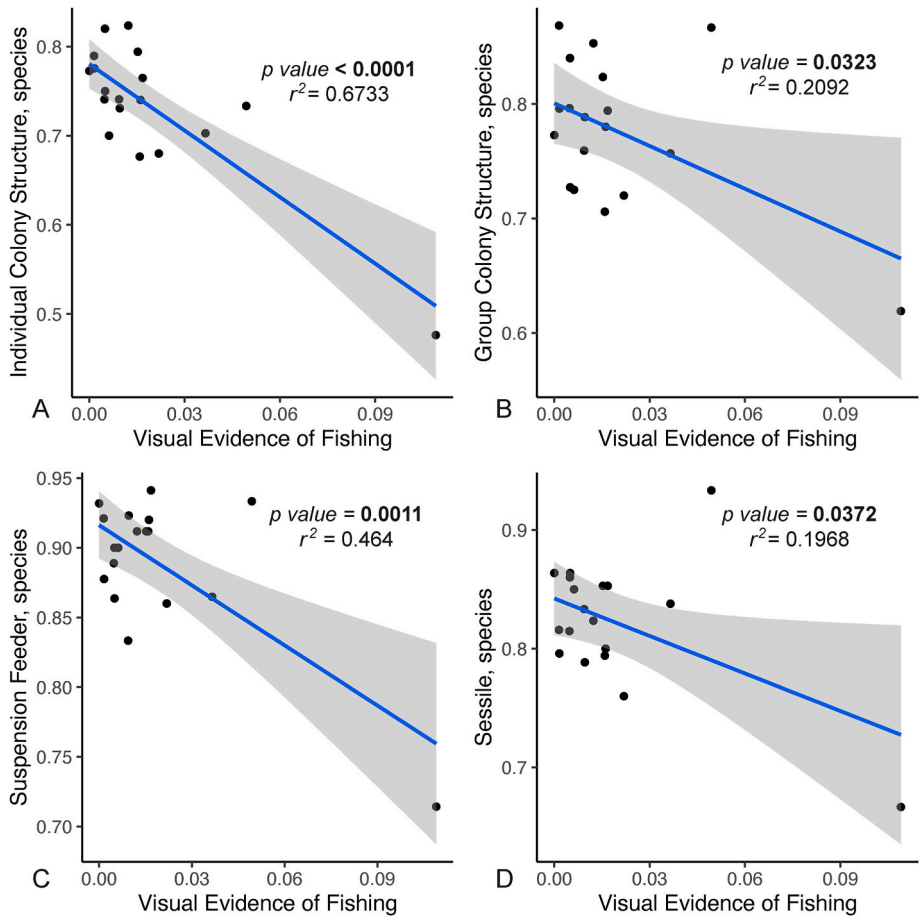

Fig. 6. Proportion of species traits, calculated as the proportion of species with trait presence within a transect, against the Visual Evidence of Fishing with p-value and r^2 in text, and 95 % confidence interval highlighted in gray. Traits include (A) Individual Colony Structure, (B) Group Colony Structure, (C) Trophic Group, (D) Mobility class. Bolded numbers indicate p-value <0.05.

Similarly, water mass was most correlated to broadscale changes in benthic assemblages at sites in the central Pacific (Auscavitch et al., 2020).

Benthic community structure is also heavily influenced by the habitat heterogeneity created by bathymetric parameters in the deep sea (reviewed in Levin et al., 2001). The correlation of community structure to bathymetric parameters, BPI finescale, BPI broadscale, and slope found here is consistent with other Pacific seamounts (Long and Baco, 2014; Mejía-Mercado et al., 2019; Mejía-Mercado and Baco, 2022, 2023; Morgan et al., 2019; Schlacher et al., 2014; Du Preez et al., 2016). Bathymetric parameters of both BPI and slope can indicate changes in features within a seamount as well as large scale seamount flanks or summits. BPI finescale may be correlated to small terraces on the flanks of Koko, whereas broadscale BPI could pertain to where the feature starts to plateau at the summit. Structures such as ridges, valleys, plateaus, terraces, and outcrops can alter the flow of the currents and increase suitability for suspension feeders, often evidenced by corals atop ridges and boulders (Buhl-Mortensen et al., 2015; Genin et al., 1986; Kennedy and Rotjan, 2022; Rogers et al., 2007). Currents can influence not only food availability (Thiem et al., 2006; Purser et al., 2010; Orejas et al., 2016; Mienis et al., 2019) but also sweep sediments away to prevent burial or clogged polyps (Genin et al., 1986). Another consideration is that aspects of bathymetry may be correlated with likelihood of trawling disturbance. The site with the greatest BPI, at 500 m SE, displayed a terraced seafloor geomorphology that might provide a level of protection to benthic megafauna from trawling. In studies of trawlable areas in the Gulf of Alaska, BPI, slope, aspect, and rugosity were key factors in determining the distribution of areas suitable for trawling (Baker et al., 2018). The influence of BPI and slope on trawlable area on Koko may therefore also contribute to the spatial variability in suitable trawling locations and therefore to the levels of Visual Evidence of Fishing observed.

A novel aspect of the current study was the incorporation of metrics of anthropogenic impact into the multivariate analysis. Intriguingly, despite the strong signal of the background natural environmental variability discussed above, the correlation of Visual Evidence of Fishing to community structure could be clearly detected, implying that fishing disturbance is having an impact not only on abundance and diversity, but also on community structure.

4.5. *Ecosystem function*

The variation between sites, in abundance, diversity, and community structure, were so significant that the ecosystem function also varied across sites on Koko. Higher evidence of fishing was correlated to reduced two-dimensional and three-dimensional structure. A similar decrease in the proportion of sessile taxa and decrease in suspension feeders was also observed on sites with greater Visual Evidence of Fishing. Given the parallel reductions in overall abundance, this pattern was likely the result of the loss of structure forming and sessile suspension feeding megafauna and not the result of new recruitment of small flexible fauna or a migration of mobile fauna.

The substantial loss of structure with increased fishing could lead to cascading effects for the community of associated organisms. The transects with the greatest Visual Evidence of Fishing contained a greater proportion of small cup corals and flexible paramuriceids and black

Table 5
Results of the Best Fit DistLM Procedure in Primer. (A) Input variables with individual correlations to the variance in the dataset. Bolded numbers indicate p-value <0.05. (B) Top 10 models calculated from the Best Fit procedure. (C) Axis correlations of the dbRDA to the model variables.

A. Marginal Tests

Variable		SS(trace)	Pseudo-F	P	Prop.
1	10-yr Chlorophyl	4041.6	1.5695	0.107	0.0893
2	Sand	1970.7	0.7287	0.755	0.0435
3	Visual Evidence of Fishing	6264.7	2.5717	**0.007**	0.1384
4	Scars	4063.3	1.5788	0.086	0.0898
5	Aspect	4396.9	1.7224	0.077	0.0971
6	Slope	9420.8	4.2079	**0.001**	0.2082
7	Curvature	3566	1.3691	0.192	0.0788
8	BPI finescale	5182.8	2.0701	0.052	0.1145
9	BPI broadscale	14534	7.5729	**0.001**	0.3212

B. Overall Best Solutions

	Selections	AIC	R^2	RSS	No. Variables
1	**3,8,9**	**135.72**	**0.5199**	**21720**	**3**
2	1,3,4,7-9	135.77	0.5691	19493	6
3	3,4,7-9	135.77	0.5691	19493	5
4	1,3,7-9	135.78	0.5690	19501	5
5	3,7-9	135.78	0.5690	19501	4
6	1,3,4,6-9	135.79	0.5688	19509	7
7	3,4,6-9	135.79	0.5688	19509	6
8	1,3,6-9	135.8	0.5686	19517	6
9	3,6-9	135.8	0.5686	19517	5
10	1,3,8,9	136.14	0.5602	19898	4

C. Biplot Scores

Variable	dbRDA1	dbRDA2	dbRDA3
Visual Evidence of Fishing	0.063	**0.971**	0.232
BPI fine	0.079	0.227	**0.971**
BPI broad	**0.995**	0.079	0.062

corals. These morphological traits, e.g., small or flexible, have been attributed to benthic megafaunal species with greater resilience to fishing disturbance on fished features or after bottom-contact fishing has occurred (reviewed in Goode et al., 2020). Unfortunately, decreased size or increased flexibility of structure forming organisms, especially corals, is directly related to decreasing numbers of associated organisms (Buhl-Mortensen and Mortensen, 2006; De Clippele et al., 2019). Furthermore, three-dimensional structure, whether a single colony or in a group structure such as a reef, creates important niches for associated species (Buhl-Mortensen et al., 2010). The structures created by coral and sponge colonies also functions as a "feeding-platform", allowing smaller invertebrate suspension feeders such as shrimps and crabs to rise above the benthic boundary layer to access food particles in the flowing currents (Buhl-Mortensen et al., 2010; De Clippele et al., 2015). The loss may also have cascading impacts on local trophic transfer as both coral reefs, living and dead structure, and sponges have been linked to nutrient regeneration and recycling, either through biofilms associated with coral skeletons (De Clippele et al., 2021; van Oevelen et al., 2018), or the "sponge loop" regenerating nutrients through diverse bacterial communities within sponge species (de Goeij et al., 2013; Rix et al., 2016). Therefore, the loss of Individual and Group Colony Structure within coral and sponge systems documented here would be expected to lead to decreased niche space and refugia for associates, likely resulting in a loss of associated biodiversity. As such, the fauna found in more impacted regions of Koko are likely to host lower associated biodiversity in comparison to sites with more structurally complex communities not removed by bottom-contact gear.

The loss of suspension feeders at impacted sites parallels the loss of this trophic group observed after the Deepwater Horizon oil spill (Nunnally et al., 2020). The megafaunal community at background sites not impacted by the spill were composed of predominantly sessile filter feeding megafauna, with both traits completely lost at impacted sites even seven years after the oil spill (Nunnally et al., 2020). These traits were replaced with increases in mobile benthic foragers, scavengers, and surface deposit feeders (Nunnally et al., 2020). However, there is no evidence for replacement of suspension feeders on Koko on sites with the greatest Visual Evidence of Fishing.

Disturbance, whether anthropogenic or natural, has been shown to decrease functional trait richness leading to decreased ecosystem functioning (reviewed in Mouillot et al., 2013). Regular trawling on soft-sediment habitats of the Mediterranean has led to altered organic matter content and carbon regeneration in comparison to less impacted sites (Pusceddu et al., 2014) highlighting the change in ecosystem functioning with changing community composition. Consistent with these patterns, the loss of functional traits observed on Koko collectively indicate substantial loss of ecosystem function proportional to increased fishing pressure. On the most impacted sites on Koko, therefore, the change in functional traits has likely led to synergistic negative effects on associated biodiversity requiring additional time for recovery.

A caveat of these analyses is that the 400 m NE site shows drastically higher values of Visual Evidence of Fishing that may bias the regression analyses. Indeed, when this site is removed from the ecosystem function models the strength of some of the correlations is reduced, although both proportional trait abundance of sessile and suspension feeding fauna remain significant ($p < 0.0005$, with r^2 values 0.45 and 0.68, Supplemental Fig. 7). Global Fishing Watch data from Morgan and Baco (2020) shows trawling activity adjacent to the 400 m NE transects. Furthermore, all images were analyzed by a single annotator, and there are three replicate transects that support the same result. Therefore, it is likely that these data are representative of the state of the ecosystem at the highest end of the range of impact levels, rather than being true outliers. Having more sites along a continuous gradient of Visual Evidence of Fishing would help to better resolve the shape and significance of the regression curves for these analyses.

4.6. *Inferences about disturbance states on Koko*

Fishing has occurred on Koko Guyot for over 60 years, with evidence of varied fishing effort spatially and temporally (Morgan and Baco, 2020). Ecological theory surrounding disturbance incorporates disturbance strength and time since disturbance event as drivers of diversity (reviewed in Viljur et al., 2022). Therefore, communities on Koko would be not only impacted by the spatial distribution and localized effort of fishing impacts, evidenced by Visual Evidence of Fishing, but also by temporal variability in fishing impacts. Disturbance can lead to several community states: a post-disturbance community that remains disturbed, a post-disturbance community that recovers to the original undisturbed state, or a post-disturbance community that recovers to an alternate state (reviewed in Lotze et al., 2011). The drivers of recovery include reduced anthropogenic disturbance but are also a function of life history and environment (Lotze et al., 2011), with the process accelerated by remnant and resilient patches of fauna that survived the disturbance event (Gunderson, 2000). Results presented here and in previous work (Baco et al., 2017, 2019, 2020, 2023a; Morgan and Baco, 2020) support the presence of all community disturbance states on Koko.

Evidence found in this study supporting a disturbed state includes transects at 400 m NE and 500 m NE with particularly low benthic megafauna abundance and diversity, and particularly high observations of derelict fishing gear, especially nets, and the presence of trawl scars. Coral abundance on Koko at the 400 m NE site resembled impacted sites on Yuryaku and Kammu, with similarly low megafaunal abundance adjacent to Visual Evidence of Fishing (Baco et al., 2020). Trait-based analyses found these sites had low structural complexity and were dominated by mobile opportunistic megafauna rather than sessile suspension feeders. These sites also had low presence of precious red corals, *H. laauense*, another potential indicator of disturbance found on fished seamounts of the HESC (Baco et al., 2023a). Support for disturbed sites

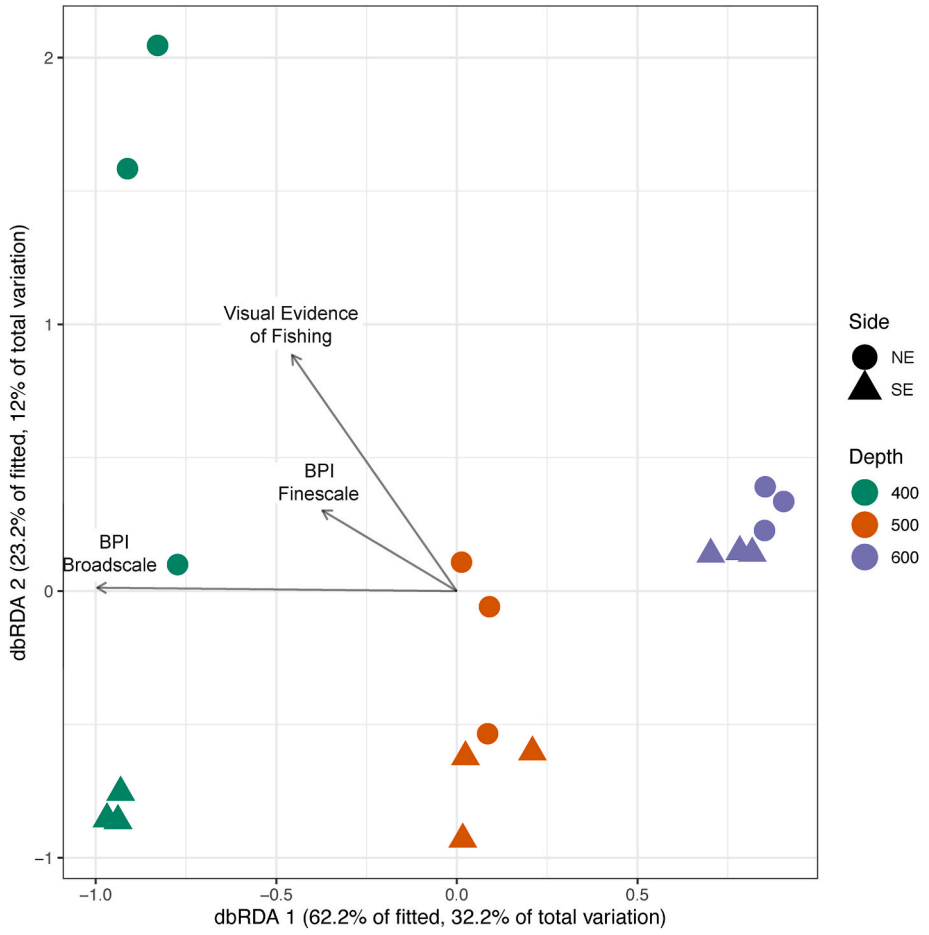

Fig. 7. Biplot of dbRDA scores for all sites on Koko, points represent transects. Color of the point indicates depth zone, while shape of the point indicates the side. (For interpretation of the references to colour in this figure legend, the reader is referred to the Web version of this article.)

on Koko is corroborated by the SAIs on seafloor communities observed on adjacent seamounts (Baco et al., 2019, 2020), resembling the loss of scleractinian reefs and associated biodiversity on fished seamounts of the South Pacific (Clark et al., 2016; Koslow et al., 2001).

Evidence from this study and past research also supports a state in the process of recovery on Koko. Baco et al. (2023a) provide some evidence for recovery on Koko based on mean coralliid size. Coralliids were significantly smaller on Koko and other trawled seamounts than on never trawled features, suggesting new recruitment or resilience of smaller individuals (Baco et al., 2023a). In addition, this study found widespread dominance of the yellow *Acanthogorgia* spp. across all sites. Paramuriceid octocorals are somewhat flexible and relatively fast growing as outlined above. Consequently, a significant colonization event for this species could lead to the observed dominance of this taxon across Koko. Therefore, the presence of the potentially faster growing yellow *Acanthogorgia* spp. at the most depauperate sites combined with high visual evidence of fishing, could indicate assemblages in the early stages of the process of recovery after disturbance. Unfortunately, this research was conducted post fishing disturbance, so it is unknown whether the *Acanthogorgia* spp. was a part of the baseline community or is an early colonizer indicating the start of the recovery process.

Evidence found in this study supporting remnant or resilient patches includes the localized patches of highly diverse and abundant megafaunal assemblages, some of which may be protected by seafloor geomorphology. These assemblages consist of large slow-growing isidids, primnoids, and patches of scleractinian reef-forming colonies, as well as precious red coral *H. laauense* colonies found on sites with fewer observations of derelict fishing gear and trawl scars. The lack of reef structure may indicate previous trawling impacts with the individual colonies representing recovering fragments or new recruitment, similar to other fished seamounts (reviewed in Goode et al., 2020), although it is also possible that reefs were not a part of the pre-disturbance community and instead small patches are consistent with the pre-disturbance community. The reef-forming species, *M. oculata* and *S. variabilis,* found on Koko are susceptible to trawling disturbance and are relatively slow growing, with linear growth rates between 4 and 9 mm/yr for *M. oculata* (Orejas et al., 2011; Lartaud et al., 2014; Chapron et al., 2020), and 0.5–3.5 mm/yr for *S. variabilis* (Fallon et al., 2014; Gammon et al., 2018). Similarly, there is evidence of slow growth rates for several of the large corals found within the localized patches of high abundance, e.g. less than 3 cm/yr in linear growth in the north Atlantic; 0.3–1 cm/yr: *Acanella arbuscula, Keratoisis ornata*; 1.2–1.36 cm/yr: *Stauropathes arctica*; 1–2.6 cm/yr: *Primnoa resedaeformis* (Sherwood and Edinger, 2009). It is therefore unlikely, with these growth rates, that the larger corals found in these patches on the SE side could be evidence of new colonization during continued disturbance, and instead are more likely to represent patches of remnant biodiversity. Similarly, the particularly high abundance and species richness at the 500 m SE site suggests reduced impacts from fishing effort. Therefore, the communities observed on Koko appear to represent a mosaic of remnant and recovering patches alongside more recently disturbed areas.

4.7. Management implications: VME presence and significant adverse impacts

Gorgonians, antipatharians, and scleractinians are found in

abundance on Koko and are recognized as VME indicators by the North Pacific Fishery Commission (NPFC). A density threshold for the designation of a VME through visual observations of VME indicators in the NPFC has not been agreed upon. However, recent work by international experts suggests VMEs can be determined for specific VME indicator groups through inspection of individual imagery (Baco et al., 2023c). Using the framework for identifying a VME from a single image designed in (Baco et al., 2023c) the presence of large VME taxa in high densities and the presence of taxa threatened by fishing pressure supports the presence of VMEs across transects on Koko.

Diverse cold-water coral and sponge patches found on Koko, whether untouched by fishing disturbance through spatial and temporal heterogeneity of fishing activity, or recovering from disturbance, are functionally significant habitats hosting individuals that can reseed impacted sites. Taxa with structure-forming traits were proportionally more abundant in sites with lower evidence of fishing. These potentially protected patches of diversity and biogenic structure increase habitat complexity providing important habitat space (Buhl-Mortensen et al., 2010; Buhl-Mortensen and Mortensen, 2006) and act as sources of propagules for recolonization of impacted areas. Similar remnant patches in other habitats are known to increase rates of recovery from disturbance, i.e., eelgrass beds (Hall et al., 2021; Johnson et al., 2021) and shallow tropical corals (reviewed in Connell et al., 1997; Gilmour et al., 1979). Therefore, the remnant and recovering patches found on Koko provide functionally significant habitat in their role as biogenic habitat formers and sources of recolonizing diversity, both of which are diagnostic characteristics of VMEs.

This is not the sole observation or support for VMEs on Koko, or the other still trawled seamounts of the HESC. Koko, Yuryaku, Kammu, and Colahan Seamounts (as well as several sites within the Papahānaumokuākea Marine National Sanctuary) support VMEs alongside evidence of SAIs from bottom contact fisheries (Baco et al., 2019, 2020). These SAIs compromise ecosystem structure and function (UNGA and Resolution adopted by the General 61/105, 2007), with examples found here including derelict fishing gear, removal of coral and sponge garden or reef habitat, and loss of biodiversity. The previous observations of VMEs and SAIs on these features should warrant protection, based on NPFC and Fisheries and Aquaculture Organization (FAO) guidelines (Baco et al., 2020), yet these features remain open to bottom-contact fishing. Here, derelict fishing gear and the presence of trawl scars, incorporated within the Visual Evidence of Fishing metric, directly correlated to a loss of ecosystem function, one of the defining components of SAIs. Decreased structural complexity through loss of Individual and Group Colony Structure, as well as reduced sessile suspension feeders has the potential to decrease nutrient regeneration and abundance of coral and sponge associated invertebrates. Therefore, this study provides further evidence of SAIs to VMEs on Koko.

5. Conclusions

Koko Guyot, a feature with over 60 years of significant bottom-contact trawling effort, hosts not only depauperate impacted megabenthic communities, but also unexpected diversity and abundance. Arranged in a mosaic of recovering, remnant, and recently disturbed sites, Koko has a surprising abundance of slow-growing and complex biogenic habitats indicative of VMEs in several areas. Overall, the richer areas on Koko are representative of other seamount communities in the Pacific, with a high abundance and diversity of octocorals as well as scleractinians, while the most impacted sites are more similar to depauperate seamounts such as seamounts within the Milwaukee Banks, Kammu and Yuryaku, with exceptionally high historical fishing effort. Heterogeneity in fishing effort seems to strongly structure Koko benthic megafaunal communities. This study found negative influences on abundance, diversity and ecosystem functioning, and changes in community structure and traits of benthic megafauna with increased evidence of fishing impacts, constituting an SAI to these VME areas. Yet among the heavily impacted sites there were also patches of large and diverse biogenic habitat formers. These patches of remnant and recovering fauna urgently need protection before they are lost, as they are likely to accelerate the recovery process in more heavily impacted areas.

CRediT authorship contribution statement

Virginia C. Biede: Writing – review & editing, Writing – original draft, Visualization, Methodology, Investigation, Formal analysis, Data curation, Conceptualization. **Nicole B. Morgan:** Writing – review & editing, Data curation. **E. Brendan Roark:** Writing – review & editing, Funding acquisition, Data curation. **Amy R. Baco:** Writing – review & editing, Supervision, Methodology, Funding acquisition, Formal analysis, Data curation, Conceptualization.

Funding

The field research and imagery collections were supported by NSF grant numbers OCE-1334652 awarded to ARB and OCE-1334675 awarded to EBR. The lead author and ARB were supported by grant OCE-1851365 awarded to ARB.

Declaration of competing interest

The authors declare that they have no known competing financial interests or personal relationships that could have appeared to influence the work reported in this paper.

Acknowledgements

The authors would like to thank the captains and crews of the *Ka'imikai-O-Kanaloa* and *Pisces IV* and *V* submersibles. There was also a large field team who collected samples and imagery including Beatriz Mejía-Mercado, Arvind Shantharam, Kelci Miller, Savannah Goode, Allison Metcalf, Kelly Klein, Julia Andrews, Travis Ferguson, Danielle Schimmenti, and Jessica Perelman. We acknowledge the work of Mauricio Aguilera-Silva on the collection of GLODAP and LDEO datasets and instruction on use of ERDDAP. Lastly, thanks to Morgan Dansby who worked on the substrate analysis for the project.

Appendix A. Supplementary data

Supplementary data to this article can be found online at https://doi.org/10.1016/j.marenvres.2025.107587.

Data availability

Data will be made available on request.

References

Althaus, F., Williams, A., Schlacher, T.A., Kloser, R.J., Green, M.A., Barker, B.A., Bax, N. J., Brodie, P., Schlacher-Hoenlinger, M.A., 2009. Impacts of bottom trawling on deep-coral ecosystems of seamounts are long-lasting. Mar. Ecol. Prog. Ser. 397, 279–294. https://doi.org/10.3354/meps08248.

Amon, D.J., Kennedy, B.R.C., Cantwell, K., Suhre, K., Glickson, D., Shank, T.M., Rotjan, R.D., 2020. Deep-Sea debris in the Central and western Pacific ocean. Front. Mar. Sci. 7, 1–16. https://doi.org/10.3389/fmars.2020.00369.

Anderson, M., Gorley, R.N., Clarke, R.K., 2008. PERMANOVA+ for PRIMER: Guide to Software and Statistical Methods. First, PRIMER-E, Plymouth.

Auscavitch, S.R., Deere, M.C., Keller, A.G., Rotjan, R.D., Timothy, M., Cordes, E.E., 2020. Oceanographic drivers of deep-sea coral species distribution and community assembly on seamounts, islands, atolls, and reefs within the Phoenix Islands Protected Area. Front. Mar. Sci. 7, 1–16. https://doi.org/10.3389/fmars.2020.00042.

Baco, A.R., 2007. Exploration for deep-sea corals on North Pacific seamounts and islands. Oceanography (Wash. D. C.) 20, 108–117.

Baco, A.R., Morgan, N., Roark, E.B., Silva, M., Shamberger, K.E.F., Miller, K., 2017. Defying dissolution: discovery of deep-sea scleractinian coral reefs in the North Pacific. Sci. Rep. 7, 1–11. https://doi.org/10.1038/s41598-017-05492-w.

Baco, A.R., Roark, E.B., Morgan, N.B., 2019. Amid fields of rubble, scars, and lost gear, signs of recovery observed on seamounts on 30- to 40-year time scales. Sci. Adv. 5. https://doi.org/10.1126/sciadv.aaw4513 eaaw4513.

Baco, A.R., Morgan, N.B., Roark, E.B., 2020. Observations of vulnerable marine ecosystems and significant adverse impacts on high seas seamounts of the Northwestern Hawaiian Ridge and Emperor Seamount Chain. Mar. Pol. 115, 103834. https://doi.org/10.1016/j.marpol.2020.103834.

Baco, A.R., Morgan, N.B., Brendan Roark, E., Biede, V., 2023a. Bottom-contact fisheries disturbance and signs of recovery of precious corals in the Northwestern Hawaiian Islands and Emperor Seamount Chain. Ecol. Indic. 148, 110010. https://doi.org/10.1016/j.ecolind.2023.110010.

Baco, A.R., Parrish, F.A., Auscavitch, S., Cairns, S., Mejia-Mercado, B.E., Biede, V., Morgan, N., Roark, E.B., Ben, Brantley W., 2023b. Deep-Sea corals of the North and Central Pacific seamounts. In: Cordes, E., Mienis, F. (Eds.), Cold-Water Coral Reefs of the World. Springer International Publishing, Cham, pp. 261–293. https://doi.org/10.1007/978-3-031-40897-7_10.

Baco, A.R., Ross, R., Althaus, F., Amon, D., Bridges, A.E.H., Brix, S., Buhl-Mortensen, P., Colaco, A., Carreiro-Silva, M., Clark, M.R., Du Preez, C., Franken, M.L., Gianni, M., Gonzalez-Mirelis, G., Hourigan, T., Howell, K., Levin, L.A., Lindsay, D.J., Molodtsova, T.N., Morgan, N., Morato, T., Mejia-Mercado, B.E., O'Sullivan, D., Pearman, T., Price, D., Robert, K., Robson, L., Rowden, A.A., Taylor, J., Taylor, M., Victorero, L., Watling, L., Williams, A., Xavier, J.R., Yesson, C., 2023c. Towards a scientific community consensus on designating Vulnerable Marine Ecosystems from imagery. PeerJ 11. https://doi.org/10.7717/peerj.16024.

Baker, P., Minzlaff, U., Schoenle, A., Schwabe, E., Hohlfeld, M., Jeuck, A., Brenke, N., Prausse, D., Rothenbeck, M., Brix, S., Frutos, I., Jörger, K.M., Neusser, T.P., Koppelmann, R., Devey, C., Brandt, A., Arndt, H., 2018. Potential contribution of surface-dwelling Sargassum algae to deep-sea ecosystems in the southern North Atlantic. Deep Sea Res 2 Top Stud Oceanogr 148, 21–34. https://doi.org/10.1016/j.dsr2.2017.10.002.

Blanca, M.J., Alarcón, R., Arnau, J., Bono, R., Bendayan, R., 2017. Non-normal data: is ANOVA still a valid option? Psicothema 29, 552–557. https://doi.org/10.7334/psicothema2016.383.

Blanca, M.J., Arnau, J., García-Castro, F.J., Alarcón, R., Bono, R., 2023. Non-normal data in repeated measures ANOVA: impact on type I error and power. Psicothema 35, 21–29. https://doi.org/10.7334/psicothema2022.292.

Bograd, S.J., Rabinovich, A.B., Leblond, P.H., Shore, J.A., 1997. Observations of seamount-attached eddies in the North Pacific. J. Geophys. Res. Oceans 102, 12441–12456. https://doi.org/10.1029/97JC00585.

Buhl-Mortensen, L., Mortensen, P.B., 2006. Distribution and diversity of species associated with deep-sea gorgonian corals off Atlantic Canada, Cold-Water Corals and Ecosystems, 849–879. https://doi.org/10.1007/3-540-27673-4_44.

Buhl-Mortensen, L., Vanreusel, A., Gooday, A.J., Levin, L.A., Priede, I.G., Buhl-Mortensen, P., Gheerardyn, H., King, N.J., Raes, M., 2010. Biological structures as a source of habitat heterogeneity and biodiversity on the deep ocean margins. Mar. Ecol. 31, 21–50. https://doi.org/10.1111/j.1439-0485.2010.00359.x.

Buhl-Mortensen, L., Olafsdottir, S.H., Buhl-Mortensen, P., Burgos, J.M., Ragnarsson, S.A., 2015. Distribution of nine cold-water coral species (Scleractinia and Gorgonacea) in the cold temperate North Atlantic: effects of bathymetry and hydrography. Hydrobiologia 759, 39–61. https://doi.org/10.1007/s10750-014-2116-x.

Chao, A., Gotelli, N.J., Hsieh, T.C., Sander, E.L., Ma, K.H., Colwell, R.K., Ellison, A.M., 2014. Rarefaction and extrapolation with Hill numbers: a framework for sampling and estimation in species diversity studies. Ecol. Monogr. 84, 45–67. https://doi.org/10.1890/13-0133.1.

Chapron, L., Le Bris, N., Durrieu de Madron, X., Peru, E., Galand, P.E., Lartaud, F., 2020. Long term monitoring of cold-water coral growth shows response to episodic meteorological events in the NW Mediterranean. Deep Sea Res. 1 Oceanogr. Res. Pap. 160, 103225. https://doi.org/10.1016/j.dsr.2020.103255.

Chassignet, E.P., Hurlburt, H.E., Smedstad, O.M., Halliwell, G.R., Hogan, P.J., Wallcraft, A.J., Baraille, R., Bleck, R., 2007. The HYCOM (HYbrid Coordinate Ocean Model) data assimilative system. J. Mar. Syst. 65, 60–83. https://doi.org/10.1016/j.jmarsys.2005.09.016.

Clague, D.A., Dalrymple, G.B., Greene, H.G., Wald, D., Kono, M., Kroenke, L.W., 1980. Bathymetry of the Emperor Seamounts. Rep. Deep Sea Drill Pro. 55, 845–849. https://doi.org/10.1017/CBO9781107415324.004.

Clague, D.A., Braga, J.C., Bassi, D., Fullagar, P.D., Renema, W., Webster, J.M., 2010. The maximum age of Hawaiian terrestrial lineages: geological constraints from Kōko Seamount. J. Biogeogr. 37, 1022–1033. https://doi.org/10.1111/j.1365-2699.2009.02235.x.

Clark, M.R., Vinnichenko, V.I., Gordon, J.D.M., Beck-bulat, G.Z., Kukharev, N.N., Alexander, F., 2007. Large-scale distant-water trawl fisheries on seamounts. In: Seamounts: Ecology, Fisheries & Conservation, pp. 361–399.

Clark, M.R., Althaus, F., Schlacher, T.A., Williams, A., Bowden, D.A., Rowden, A.A., 2016. The impacts of deep-sea fisheries on benthic communities: a review. ICES (Int. Counc. Explor. Sea) J. Mar. Sci. 73, i51–i69. https://doi.org/10.1093/icesjms/fsv123.

Clark, M.R., Bowden, D.A., Rowden, A.A., Stewart, R., 2019. Little evidence of benthic community resilience to bottom trawling on seamounts after 15 years. Front. Mar. Sci. 6. https://doi.org/10.3389/fmars.2019.00063.

Colaço, A., Rapp, H.T., Campanyà-Llovet, N., Pham, C.K., 2022. Bottom trawling in sponge grounds of the Barents Sea (Arctic Ocean): a functional diversity approach. Deep Sea Res. 1 Oceanogr. Res. Pap. 183. https://doi.org/10.1016/j.dsr.2022.103742.

Connell, J.H., 1978. Diversity in tropical rain forests and coral reefs. Hefte Unfallheilkd. 199, 1302–1310.

Connell, J.H., Hughes, T.P., Wallace, C.C., 1997. A 30-year study of coral abundance, recruitment, and disturbance at several scales in space and time. Ecol. Monogr. 67, 461–488. https://doi.org/10.1890/0012-9615(1997)067[0461:AYSOCA]2.0.CO;2.

Cryer, M., Hartill, B., O'Shea, S., 2002. Modification of marine benthos by trawling: toward a generalization for the deep ocean? Ecol. Appl. 12, 1824–1839.

Dautova, T.N., Galkin, S.V., Tabachnik, K.R., Minin, K.V., Kireev, P.A., Moskovtseva, A. V., Adrianov, A.V., 2019. The first data on the structure of vulnerable marine ecosystems of the Emperor Chain seamounts: indicator taxa, landscapes, and biogeography. Russ. J. Mar. Biol. 45, 408–417. https://doi.org/10.1134/S1063074019060026.

Davies, T.A., Wilde, P., Clague, D.A., 1972. Koko Seamount: a major guyot at the southern end of the Emperor Seamounts. Mar. Geol. 13, 311–336.

De Cáceres, M., Legendre, P., 2009. Associations between species and groups of sites: indices and statistical inference. Ecology 90, 3566–3574. https://doi.org/10.1890/08-1823.1.

De Cáceres, M., Legendre, P., Moretti, M., 2010. Improving indicator species analysis by combining groups of sites. Oikos 119, 1674–1684. https://doi.org/10.1111/j.1600-0706.2010.18334.x.

De Clippele, L.H., Buhl-Mortensen, P., Buhl-Mortensen, L., 2015. Fauna associated with cold water gorgonians and sea pens. Cont. Shelf Res. 105, 67–78. https://doi.org/10.1016/j.csr.2015.06.007.

De Clippele, L.H., Huvenne, V.A.I., Molodtsova, T.N., Roberts, J.M., 2019. The diversity and ecological role of non-scleractinian corals (Antipatharia and Alcyonacea) on scleractinian cold-water coral mounds. Front. Mar. Sci. 6, 1–16. https://doi.org/10.3389/fmars.2019.00184.

De Clippele, L.H., van der Kaaden, A.-S., Maier, S.R., de Froe, E., Roberts, J.M., 2021. Biomass mapping for an improved understanding of the contribution of cold-water coral carbonate mounds to C and N cycling. Front. Mar. Sci. 8. https://doi.org/10.3389/fmars.2021.721062.

de Goeij, J.M., van Oevelen, D., Vermeij, M.J.A., Osinga, R., Middelburg, J.J., de Goeij, A.F.P.M., Admiraal, W., 2013. Surviving in a marine desert: the sponge loop retains resources within coral reefs. Science 342, 108–110. https://doi.org/10.1126/science.1241981.

Du Preez, C., Curtis, J.M.R., Clarke, M.E., 2016. The structure and distribution of benthic communities on a shallow seamount (Cobb Seamount, Northeast Pacific Ocean). PLoS One 11, 1–29. https://doi.org/10.1371/journal.pone.0165513.

Du Preez, C., Swan, K.D., Curtis, J.M.R., 2020. Cold-water corals and other vulnerable biological structures on a North Pacific seamount after half a century of fishing. Front. Mar. Sci. 7. https://doi.org/10.3389/fmars.2020.00017.

Fallon, S.J., Thresher, R.E., Adkins, J., 2014. Age and growth of the cold-water scleractinian Solenosmilia variabilis and its reef on SW Pacific seamounts. Coral Reefs 33, 31–38. https://doi.org/10.1007/s00338-013-1097-y.

FAO, 2009. International Guidelines: Management of Deep-Sea Fisheries in the High Seas.

Feir-Walsh, B.J., Toothaker, L.E., 1974. An empirical comparison of the ANOVA F-test, normal scores test and Kruskal-Wallis test under violation of assumptions. Educ. Psychol. Meas. 34, 789–799.

Freiwald, A., Fossså, J.H., Grehan, A., Koslow, T., Roberts, J.M., 2004. Cold Water Coral Reefs: Out of Sight-No Longer Out of Mind. UNEP-WCMC, Cambridge, UK. https://resources.unep-wcmc.org/products/WCMC_RT145.

Gammon, M.J., Tracey, D.M., Marriott, P.M., Cummings, V.J., Davy, S.K., 2018. The physiological response of the deep- sea coral Solenosmilia variabilis to ocean acidification. PeerJ 2018, 1–24. https://doi.org/10.7717/peerj.5236.

GEBCO Bathymetric Compilation Group, 2021. The GEBCO_2021 Grid. https://doi.org/10.5285/c6612cbe-50b3-0cff-e053-6c86abc09f8f, 2021.

Genin, A., Dayton, P.K., Lonsdale, P.F., Spiess, F.N., 1986. Corals on seamount peaks provide evidence of current acceleration over deep-sea topography. Nature 322, 59–61. https://doi.org/10.1038/322059a0.

Gilman, E., Musyl, M., Suuronen, P., Chaloupka, M., Gorgin, S., Wilson, J., Kuczenski, B., 2021. Highest risk abandoned, lost and discarded fishing gear. Sci. Rep. 11. https://doi.org/10.1038/s41598-021-86123-3.

Gilmour, J.P., Smith, L.D., Heyward, A.J., Baird, A.H., Pratchett, M.S., 1979. Recovery of an isolated coral reef system following severe disturbance. Science 340, 69–71. https://doi.org/10.1126/science.1232310, 2013.

Goode, S.L., Rowden, A.A., Bowden, D.A., Clark, M.R., 2020. Resilience of seamount benthic communities to trawling disturbance. Mar. Environ. Res. 161. https://doi.org/10.1016/j.marenvres.2020.105086.

Goode, S.L., Rowden, A.A., Bowden, D.A., Clark, M.R., Stephenson, F., 2021. Fine-scale mapping of mega-epibenthic communities and their patch characteristics on two New Zealand seamounts. Front. Mar. Sci. 8. https://doi.org/10.3389/fmars.2021.765407.

Grigg, R.W., 2002. Precious corals in Hawaii: discovery of a new bed and revised management measures for existing beds. Mar. Fish. Rev. 64, 13–20.

Gunderson, L.H., 2000. Ecological resilience–in theory and application. Annu. Rev. Ecol. Systemat. 31, 425–439. https://www.jstor.org/stable/221739?seq=1&cid=pdf-.

Hall, M.O., Bell, S.S., Furman, B.T., Durako, M.J., 2021. Natural recovery of a marine foundation species emerges decades after landscape-scale mortality. Sci. Rep. 11, 1–10. https://doi.org/10.1038/s41598-021-86160-y.

Hijmans, R.J., 2025. Raster: geographic data analysis and modeling. https://CRAN.R-project.org/package=raster.

Hill, M.O., 1973. Diversity and evenness: a unifying notation and its consequences. Ecology 54, 427–432.

Johnson, A.J., Shields, E.C., Kendrick, G.A., Orth, R.J., 2021. Recovery dynamics of the seagrass zostera marina following mass mortalities from two extreme climatic events. Estuaries Coasts 44, 535–544. https://doi.org/10.1007/s12237-020-00816-y.

Kennedy, B., Rotjan, R., 2022. The Impact of Geological Feature Shape on the Abundance and Diversity of Deep Sea Corals. Authorea. https://doi.org/10.22541/au.167170187.77435246/v1.
Kerry, C.R., Exeter, O.M., Witt, M.J., 2022. Monitoring global fishing activity in proximity to seamounts using automatic identification systems. Fish Fish. 23, 733–749. https://doi.org/10.1111/faf.12647.
Koslow, J.A., Gowlett-Holmes, K., Lowry, J.K., O'Hara, T., Poore, G.C.B., Williams, A., 2001. Seamount benthic macrofauna off southern Tasmania: community structure and impacts of trawling. Mar. Ecol. Prog. Ser. 213, 111–125. https://doi.org/10.3354/meps213111.
Lartaud, F., Pareige, S., de Rafelis, M., Feuillassier, L., Bideau, M., Peru, E., De la Vega, E., Nedoncelle, K., Romans, P., Le Bris, N., 2014. Temporal changes in the growth of two Mediterranean cold-water coral species, in situ and in aquaria. Deep Sea Res 2 Top Stud Oceanogr 99, 64–70. https://doi.org/10.1016/j.dsr2.2013.06.024.
Lauvset, S.K., Lange, N., Tanhua, T., Bittig, H.C., Olsen, A., Kozyr, A., Álvarez, M., Becker, S., Brown, P.J., Carter, B.R., Cotrim Da Cunha, L., Feely, R.A., Van Heuven, S., Hoppema, M., Ishii, M., Jeansson, E., Jutterström, S., Jones, S.D., Karlsen, M.K., Lo Monaco, C., Michaelis, P., Murata, A., Pérez, F.F., Pfeil, B., Schirnick, C., Steinfeldt, R., Suzuki, T., Tilbrook, B., Velo, A., Wanninkhof, R., Woosley, R.J., Key, R.M., 2021. An updated version of the global interior ocean biogeochemical data product, GLODAPv2.2021. Earth Syst. Sci. Data 13, 5565–5589. https://doi.org/10.5194/essd-13-5565-2021.
Levin, L.A., Etter, R.J., Rex, M.A., Gooday, A.J., Smith, C.R., Pineda, J., Stuart, C.T., Hessler, R.R., Pawson, D., 2001. Environmental influences on regional deep-sea species diversity. Annu. Rev. Ecol. Systemat. 32, 51–93.
Li, D., 2018. hillR: taxonomic, functional, and phylogenetic diversity and similarity through Hill Numbers. J. Open Source Softw. 3, 1041. https://doi.org/10.21105/joss.01041.
Long, D.J., Baco, A.R., 2014. Rapid change with depth in megabenthic structure-forming communities of the Makapu'u deep-sea coral bed. Deep Sea Res 2 Top Stud Oceanogr 99, 158–168. https://doi.org/10.1016/j.dsr2.2013.05.032.
Lotze, H.K., Coll, M., Magera, A.M., Ward-Paige, C., Airoldi, L., 2011. Recovery of marine animal populations and ecosystems. Trends Ecol. Evol. 26, 595–605. https://doi.org/10.1016/j.tree.2011.07.008.
MacArthur, R.H., MacArthur, J.W., 1961. On bird species diversity. Ecology 42, 594–598. https://www.jstor.org/stable/1932254. (Accessed 27 August 2025).
Mejía-Mercado, B.E., Baco, A.R., 2022. Characterization and spatial variation of the deep-sea fish assemblages on Pioneer Bank, Northwestern Hawaiian Islands. Mar. Ecol. Prog. Ser. 692, 99–118. https://doi.org/10.3354/meps14071.
Mejía-Mercado, B.E., Baco, A.R., 2023. Horizontal distribution of benthic and demersal fish assemblages on three seamounts in the Papahānaumokuākea Marine National Monument. Deep Sea Res. Oceanogr. Res. Pap. 195, 104003.
Mejía-Mercado, B.E., Mundy, B., Baco, A.R., 2019. Variation in the structure of the deep-sea fish assemblages on Necker Island, Northwestern Hawaiian Islands. Deep Sea Res. Oceanogr. Res. Pap. 152, 103086. https://doi.org/10.1016/j.dsr.2019.103086.
Mienis, F., Bouma, T.J., Witbaard, R., van Oevelen, D., Duineveld, G.C.A., 2019. Experimental assessment of the effects of coldwater coral patches on water flow. Mar. Ecol. Prog. Ser. 609, 101–117.
Miyamoto, M., Kiyota, M., Hayashibara, T., Nonaka, M., Imahara, Y., Tachikawa, H., 2017. Megafaunal composition of cold-water corals and other deep-sea benthos in the southern Emperor Seamounts area, North Pacific Ocean, Galaxea. J. Coral Reef. Stud. 19, 19–30. https://doi.org/10.3755/galaxea.19.1_19.
Morgan, N.B., Baco, A.R., 2020. Recent fishing footprint of the high-seas bottom trawl fisheries on the Northwestern Hawaiian Ridge and Emperor Seamount Chain: a finer-scale approach to a large-scale issue. Ecol. Indic. 121. https://doi.org/10.1016/j.ecolind.2020.107051.
Morgan, N.B., Cairns, S., Reiswig, H., Baco, A.R., 2015. Benthic megafaunal community structure of cobalt-rich manganese crusts on Necker Ridge. Deep Sea Res. Oceanogr. Res. Pap. 104, 92–105. https://doi.org/10.1016/j.dsr.2015.07.003.
Morgan, N.B., Goode, S., Roark, E.B., Baco, A.R., 2019. Fine scale assemblage structure of benthic invertebrate megafauna on the North Pacific seamount Mokumanamana. Front. Mar. Sci. 6. https://doi.org/10.3389/fmars.2019.00715.
Morris, K.J., Bett, B.J., Durden, J.M., Huvenne, V.A.I., Milligan, R., Jones, D.O.B., McPhail, S., Robert, K., Bailey, D.M., Ruhl, H.A., 2014. A new method for ecological surveying of the abyss using autonomous underwater vehicle photography. Limnol Oceanogr. Methods 12, 795–809. https://doi.org/10.4319/lom.2014.12.795.
Mouillot, D., Graham, N.A.J., Villéger, S., Mason, N.W.H., Bellwood, D.R., 2013. A functional approach reveals community responses to disturbances. Trends Ecol. Evol. 28, 167–177. https://doi.org/10.1016/j.tree.2012.10.004.
NASA Goddard Space Flight Center, Ocean Ecology Laboratory, Ocean Biology Processing Group, Moderate-Resolution Imaging Spectroradiometer (MODIS) Aqua. AQUA MODIS Level-3 Mapped Chlorophyll (CHL), Version 2022.0, (n.d.).
Nunnally, C.C., Benfield, M.C., McClain, C.R., 2020. Trait-based diversity of deep-sea benthic megafauna communities near the Deepwater Horizon oil spill site. Mar. Ecol. 41. https://doi.org/10.1111/maec.12611.
Oksanen, J., Blanchet, F.G., Friendly, M., Kindt, R., Legendre, P., McGlinn, D., Minchin, P.R., O'Hara, R.B., Simpson, G.L., Solymos, P., Stevens, H.H., Wagner, H., Szoecs, E., 2019. Vegan: community ecology package. R packag. version 2.5–6. https://doi.org/10.1016/0169-5347(88)90124-3.
Orejas, C., Ferrier-Pagès, C., Reynaud, S., Gori, A., Beraud, E., Tsounis, G., Allemand, D., Gili, J., 2011. Long-term growth rates of four Mediterranean cold-water coral species maintained in aquaria. Mar. Ecol. Prog. Ser. 429, 57–65. https://doi.org/10.3354/meps09104.
Orejas, C., Gori, A., Rad-Menéndez, C., Last, K.S., Davies, A.J., Beveridge, C.M., Sadd, D., Kiriakoulakis, K., Witte, U., Roberts, J.M., 2016. The effect of flow speed and food size on the capture efficiency and feeding behaviour of the cold-water coral Lophelia pertusa. J. Exp. Mar. Biol. Ecol. 481, 34–40. https://doi.org/10.1016/j.jembe.2016.04.002.
Parrish, F., 2007. Density and habitat of three deep-sea corals in the lower Hawaiian chain. Bull. Mar. Sci. 81, 185–194.
Parrish, F.A., Boland, R.C., 2004. Habitat and reef-fish assemblages of banks in the Northwestern Hawaiian Islands. Mar. Biol. 144, 1065–1073. https://doi.org/10.1007/s00227-003-1288-0.
Pierce, D., 2025. ncdf4: interface to unidata netCDF (version 4 or earlier) format data files. https://CRAN.R-project.org/package=ncdf4.
Puig, P., Canals, M., Company, J.B., Martín, J., Amblas, D., Lastras, G., Palanques, A., Calafat, A.M., 2012. Ploughing the deep sea floor. Nature 489, 286. https://doi.org/10.1038/nature11410.
Purser, A., Larsson, A.I., Thomsen, L., van Oevelen, D., 2010. The influence of flow velocity and food concentration on Lophelia pertusa (Scleractinia) zooplankton capture rates. J. Exp. Mar. Biol. Ecol. 395, 55–62. https://doi.org/10.1016/j.jembe.2010.08.013.
Pusceddu, A., Bianchelli, S., Martín, J., Puig, P., Palanques, A., Masqué, P., Danovaro, R., 2014. Chronic and intensive bottom trawling impairs deep-sea biodiversity and ecosystem functioning. Proc. Natl. Acad. Sci. U. S. A. 111, 8861–8866. https://doi.org/10.1073/pnas.1405454111.
R Core Team, 2022. R: A Language and Environment for Statistical Computing.
Rényi, A., 1961. On Measures of Entropy and Information, Fourth Berkeley Symposium 4, 547–561.
Rix, L., De Goeij, J.M., Mueller, C.E., Struck, U., Middelburg, J.J., Van Duyl, F.C., Al-Horani, F.A., Wild, C., Naumann, M.S., Van Oevelen, D., 2016. Coral mucus fuels the sponge loop in warm-and cold-water coral reef ecosystems. Sci. Rep. 6, 1–11. https://doi.org/10.1038/srep18715.
Rogers, A.D., 2018. The biology of seamounts: 25 years on. Adv. Mar. Biol. 79, 137–224. https://doi.org/10.1016/bs.amb.2018.06.001.
Rogers, A.D., Baco, A., Griffi, H., Hart, T., 2007. Corals on seamounts. In: Seamounts: Ecology, Conservation and Management, pp. 141–170.
Schlacher, T.A., Baco, A.R., Rowden, A.A., O'Hara, T.D., Clark, M.R., Kelley, C., Dower, J.F., 2014. Seamount benthos in a cobalt-rich crust region of the central Pacific: conservation challenges for future seabed mining. Divers. Distrib. 20, 491–502. https://doi.org/10.1111/ddi.12142.
Schneider, C.A., Rasband, W.S., Eliceiri, K.W., 2012. NIH Image to ImageJ: 25 years of image analysis. Nat. Methods 9, 671.
Shapiro, S.S., Wilk, M.B., 1965. An analysis of variance test for normality (complete samples). Biometrika 52, 591–611. https://academic.oup.com/biomet/article-abstract/52/3-4/591/336553.
Sharp, W.D., Clague, D.A., 1979. 50-Ma initiation of Hawaiian-emperor bend records major change in Pacific plate motion. Science 313, 1281–1284, 2006.
Sherwood, O.A., Edinger, E.N., 2009. Ages and growth rates of some deep-sea gorgonian and antipatharian corals of Newfoundland and Labrador. Can. J. Fish. Aquat. Sci. 66, 142–152. https://doi.org/10.1038/nature12829.
Stelzenmüller, V., Rogers, S.I., Mills, C.M., 2008. Spatio-temporal patterns of fishing pressure on UK marine landscapes, and their implications for spatial planning and management. ICES (Int. Counc. Explor. Sea) J. Mar. Sci. 65, 1081–1091. https://doi.org/10.1093/icesjms/fsn073.
Stone, R.P., 2006. Coral habitat in the Aleutian Islands of Alaska : depth distribution , fine-scale species associations , and fisheries interactions. Coral Reefs 25, 229–238. https://doi.org/10.1007/s00338-006-0091-z.
Takahashi, T., Sutherland, S.C., Chipman, D.W., Goddard, J.G., Ho, C., 2014. Climatological distributions of pH, pCO2, total CO2, alkalinity, and CaCO3 saturation in the global surface ocean, and temporal changes at selected locations. Mar. Chem. 164, 95–125. https://doi.org/10.1016/j.marchem.2014.06.004.
Thiem, Ø., Ravagnan, E., Fosså, J.H., Berntsen, J., 2006. Food supply mechanisms for cold-water corals along a continental shelf edge. J. Mar. Syst. 60, 207–219. https://doi.org/10.1016/j.jmarsys.2005.12.004.
Tóthmérész, B., 1995. Comparison of different methods for diversity ordering. J. Veg. Sci. 6, 283–290. https://doi.org/10.2307/3236223.
Tsounis, G., Rossi, S., Grigg, R., Santagelo, G., Bramanti, L., Gili, J.-M., 2010. The exploitation and conservation of precious corals. Oceanogr. Mar. Biol. Annu. Rev. 48, 161–212.
Uchida, R.N., Hayasi, S., Boehlert, G.W., 1986. Environment and Resources of Seamounts in the North Pacific National Oceanic and Atmospheric Administration. North. NOAA Technical Report NMFS 43. https://spo.nmfs.noaa.gov/content/tr-43-environment-and-resources-seamounts-north-pacific.
UNGA, Resolution adopted by the General 61/105, 2007. Sustainable Fisheries, Including through the 1995 Agreement for the Implementation of the Provisions of the United Nations Convention on the Law of the Sea of 10 December 1982 Relating to the Conservation and Management of Straddling Fish Stocks and Highly Migratory Fish Stocks, and Related Instruments.
van Oevelen, D., Duineveld, G.C.A., Lavaleye, M.S.S., Kutti, T., Soetaert, K., 2018. Trophic structure of cold-water coral communities revealed from the analysis of tissue isotopes and fatty acid composition. Mar. Biol. Res. 14, 287–306. https://doi.org/10.1080/17451000.2017.1398404.
Vastano, A.C., Hagan, D.E., McNally, G.J., 1985. Lagrangian observations of surface circulation at the Emperor Seamount Chain. J. Geophys. Res. 90, 3325. https://doi.org/10.1029/jc090ic02p03325.
Victorero, L., Robert, K., Robinson, L.F., Taylor, M.L., Huvenne, V.A.I., 2018. Species replacement dominates megabenthos beta diversity in a remote seamount setting. Sci. Rep. 8. https://doi.org/10.1038/s41598-018-22296-8.
Viljur, M.L., Abella, S.R., Adámek, M., Alencar, J.B.R., Barber, N.A., Beudert, B., Burkle, L.A., Cagnolo, L., Campos, B.R., Chao, A., Chergui, B., Choi, C.Y., Cleary, D.F.

R., Davis, T.S., Dechnik-Vázquez, Y.A., Downing, W.M., Fuentes-Ramirez, A., Gandhi, K.J.K., Gehring, C., Georgiev, K.B., Gimbutas, M., Gongalsky, K.B., Gorbunova, A.Y., Greenberg, C.H., Hylander, K., Jules, E.S., Korobushkin, D.I., Köster, K., Kurth, V., Lanham, J.D., Lazarina, M., Leverkus, A.B., Lindenmayer, D., Marra, D.M., Martín-Pinto, P., Meave, J.A., Moretti, M., Nam, H.Y., Obrist, M.K., Petanidou, T., Pons, P., Potts, S.G., Rapoport, I.B., Rhoades, P.R., Richter, C., Saifutdinov, R.A., Sanders, N.J., Santos, X., Steel, Z., Tavella, J., Wendenburg, C., Wermelinger, B., Zaitsev, A.S., Thorn, S., 2022. The effect of natural disturbances on forest biodiversity: an ecological synthesis. Biol. Rev. 97, 1930–1947. https://doi.org/10.1111/brv.12876.

Waller, R., Watling, L., Auster, P., Shank, T., 2007. Anthropogenic impacts on the corner rise seamounts, north-west Atlantic ocean. J. Mar. Biol. Assoc. U. K. 87, 1075–1076. https://doi.org/10.1017/S0025315407057785.

Watling, L., Norse, E.A., 1998. Disturbance of the seabed by mobile fishing gear: a comparison to forest clearcutting. Conserv. Biol. 12, 1180–1197. https://doi.org/10.1046/j.1523-1739.1998.0120061180.x.

Wentworth, C.K., 1922. A scale of grade and class terms for clastic sediments. J. Geol. 30, 377–392. https://doi.org/10.1086/622910.

Wickham, H., 2023. Httr: tools for working with URLs and HTTP. https://CRAN.R-project.org/package=httr.

Williams, A., Koslow, J.A., Last, P.R., 2001. Diversity, density and community structure of the demersal fish fauna of the continental slope off Western Australia (20 to 35°S). Mar. Ecol. Prog. Ser. 212, 247–263. https://doi.org/10.3354/meps212247.

Williams, A., Schlacher, T.A., Rowden, A.A., Althaus, F., Clark, M.R., Bowden, D.A., Stewart, R., Bax, N.J., Consalvey, M., Kloser, R.J., 2010. Seamount megabenthic assemblages fail to recover from trawling impacts. Mar. Ecol. 31, 183–199. https://doi.org/10.1111/j.1439-0485.2010.00385.x.

Wilson, C., Robinson, D., Simons, R.A., 2020. Erddap: providing easy access to remote sensing data for scientists and students. In: International Geoscience and Remote Sensing Symposium (IGARSS). Institute of Electrical and Electronics Engineers Inc., pp. 3207–3210. https://doi.org/10.1109/IGARSS39084.2020.9323962

Yoklavich, M.M., Laidig, T.E., Graiff, K., Elizabeth Clarke, M., Whitmire, C.E., 2018. Incidence of disturbance and damage to deep-sea corals and sponges in areas of high trawl bycatch near the California and Oregon border. Deep Sea Res 2 Top Stud Oceanogr 150, 156–163. https://doi.org/10.1016/j.dsr2.2017.08.005.